Association Euratom - Risø National Laboratory annual progress report 1996

Lynov, Jens-Peter; Singh, Bachu Narain

Publication date:
1997

Document Version
Publisher's PDF, also known as Version of record

Association Euratom - Risø National Laboratory Annual Progress Report 1996

Risø-R-990(EN)

Edited by J.P. Lynov and B.N. Singh

Risø National Laboratory, Roskilde, Denmark
May 1997

Abstract The programme of the Research Unit of the Fusion Association Euratom - Risø National Laboratory covers work in fusion plasma physics and in fusion technology. The fusion plasma physics group has activities within development of laser diagnostics for fusion plasmas and studies of nonlinear dynamical processes related to electrostatic turbulence and turbulent transport in magnetised plasmas. The activities in technology cover investigations of radiation damage of fusion reactor materials. These activities contribute to the Next Step, the Long-term and the Underlying Fusion Technology programme. A summary is presented of the results obtained in the Research Unit during 1996.

ISBN 87-550-2312-6
ISSN 0106-2840
ISSN 1396-3449

Grafisk Service • Risø • 1997

Contents

1. Preface

The activities in the Research Unit cover two main areas:

Fusion Plasma Physics which includes:

- *Laser plasma diagnostics.* Development of a new two-point collective scattering diagnostic for spatially localised turbulence measurements. In collaboration with IPP Garching this diagnostic has been installed on the W7-AS stellarator and initial measurements are in progress.
- *Nonlinear dynamics of fusion plasmas*. For the interpretation of the results from the laser diagnostic, extensive computer simulations are carried out of the plasma density fluctuations under various types of electrostatic turbulence. This simulations are also used for studies of coherent structures and their influence on turbulent transport.

Fusion Technology which includes:

- Experimental and theoretical investigations of the effects of irradiation on the microstructural evolution and on the physical and mechanical properties of metals and alloys relevant to the Next Step, the Long Term and Underlying Fusion Technology Programme.

2. Fusion Plasma Physics

2.1 Introduction

The activities in this area have been carried out under the Plasma Physics and Fluid Dynamics Programme in the Optics and Fluid Dynamics Department. The main objective of the research is to contribute to the understanding of turbulent transport in fusion plasmas. In the work towards this objective, the programme interacts with other activities in the department in the fields of optics and fluid dynamics to the mutual scientific benefit of the projects involved.

A new laser-based diagnostic with increased spatial resolution has been developed for studies of turbulent density fluctuations. In collaboration with IPP Garching, this diagnostic was installed on the W7-AS stellarator experiment in 1996. Initial measurements are currently in progress.

The interpretation of the results from the measurements is being supported by extensive computer simulations of the plasma density fluctuations under various types of electrostatic turbulence. These simulations, which are focused on addressing physical conditions at the plasma edge and in the scrape-off layer, are also used for fundamental studies of the generation and dynamical evolution of highly nonlinear, coherent structures and of the influence of such structures on the turbulent transport.

In this report, a brief description is included of some external projects which are derived from the main scientific programme:

- *Pellet injectors*. After the delivery of two eight-shot hydrogen/deuterium pellet injectors to ENEA (FTU and RFX) further research and development in this area has been terminated. However, some technical support to the groups with Risø-made pellet injectors is continued.
- *Industrial impact*. As a spin-off from the work on laser diagnostics, a new method for remote measurement of wind velocity for feed forward control of wind turbines has been devised and a patent application submitted. The work is being performed in collaboration with two industrial companies.
- *Public relations*. In 1996, the Fusion EXPO exhibition was on display in Denmark and received a very good public response.

2.2 Laser Plasma Diagnostics

2.2.1 Collective scattering turbulence diagnostic at the W7-AS stellarator

M. Saffman, B. Sass, W. Svendsen, J. Thorsen, W. Junker (until 31 March), and H. Larsen (Engineering and Computer Department)

Preparation of a two-point collective scattering diagnostic for spatially localized turbulence measurements was completed in 1996, and the instrument was installed at the W7-AS stellarator experiment at the Institute for Plasma Physics in Garching in July-August 1996. The instrument, which is based on a two-point correlation measurement technique, has been designed to give enhanced spatial resolution of large scale turbulence. Initial measurements with the diagnostic are currently in progress.

The diagnostic, as installed at the W7-AS experiment, is a complex system comprised of mechanical, optical, electronic, and computer components. A detailed description of the system design has been given in [1]. We describe here the primary features of the installed system. The optical train includes a transmitter table with 25 W CO_2 laser and beam forming optics located in the basement underneath the torus, and a receiving table mounted on top of the torus. The transmitting and receiving tables installed at the W7-AS are shown in Figure 1. The optical path length between the transmitting and receiving tables is approximately 9 meters, with communication between the two tables via radiophones, since there is no direct line of sight.

The optical access and mechanical mounting has been designed to allow translation of the measurement volume throughout a large portion of the plasma cross-section. The four optical beams (two strong primary beams, and two local oscillator beams) traverse along a vertical chord through the plasma. Optical access is through 200 mm diameter ZnSe windows located on lower and upper torus ports separated by 2 M. Large diameter windows have been mounted to enable radial adjustment of the measurement volume in the plasma by up to +/- 5cm. The radial adjustment is achieved by tilting mirrors located below and above the plasma. Continuous vertical adjustment from 60 cm below to 60 cm above the plasma midplane has been achieved by mounting the primary focusing and receiving lenses on long travel translation stages. The measurement direction in the horizontal plane can be varied continuously by rotation of dove prisms located on the transmitting and receiving tables. The combined effect of the available adjustments is that transport along both radial and poloidal directions can be investigated.

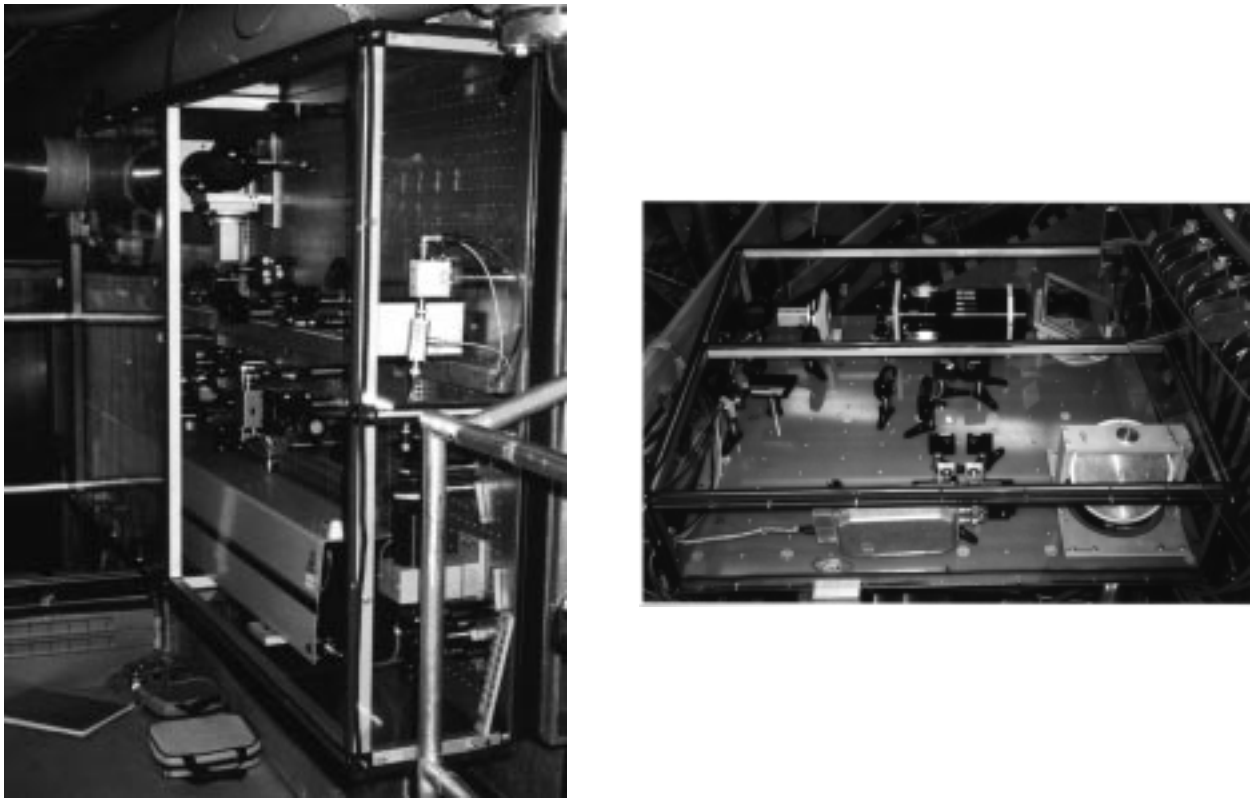

Figure 1. Transmitter (left) and receiver (right) optical tables. The infrared beams exit the transmitter table towards the torus through the aluminum duct on the upper left corner of the transmitter table. The beams are aligned to the receiver table by the large mirror on the lower right corner of the table.

The electronics consists of a primary rack located next to the transmitting table, and a smaller rack located next to the receiving table. Data acquisition is via a dedicated dual-channel, digital quadrature demultiplexer designed and built by Risø's Engineering and Computer Department. The quadrature demultiplexer is contained on a single PCI card located in a Pentium computer in the primary electronics rack. Digitized data is transferred directly to the computers main memory which has been expanded to 80 Mbytes to allow for up to 0.75 sec. of two-channel 16 MHz bandwidth quadrature data. Power spectra and correlations are calculated off-line between plasma discharges. Data acquisition and mechanical adjustments are controlled remotely from a computer in the W7-AS control room. Connection to the computer in the torus hall is via an optical ethernet link.

Initial tests concentrated on verifying mechanical stability and susceptibility to noise pickup from other electronic equipment in the torus hall. Mechanical stability has been investigated by intentionally modulating the local oscillator beams at 3 kHz and measuring the detected signal levels. Initial results indicate acceptable mechanical stability during a plasma discharge, as well as good long term mechanical stability. The system maintained good mechanical alignment during the 6 week summer shutdown of W7-AS from August to September.

Susceptibility to noise pickup has been more troublesome, due to several factors. The detected signals receive a high level of electronic gain to match them to the sensitivity of the quadrature demultiplexer, and there is about 25 m of cable between the detectors and the quadrature demultiplexer. Initial measurements showed unacceptably high levels of parasitic pickup. This necessitated improvements to the electromagnetic shielding used for the detectors and preamplifiers which were completed in December 1996.

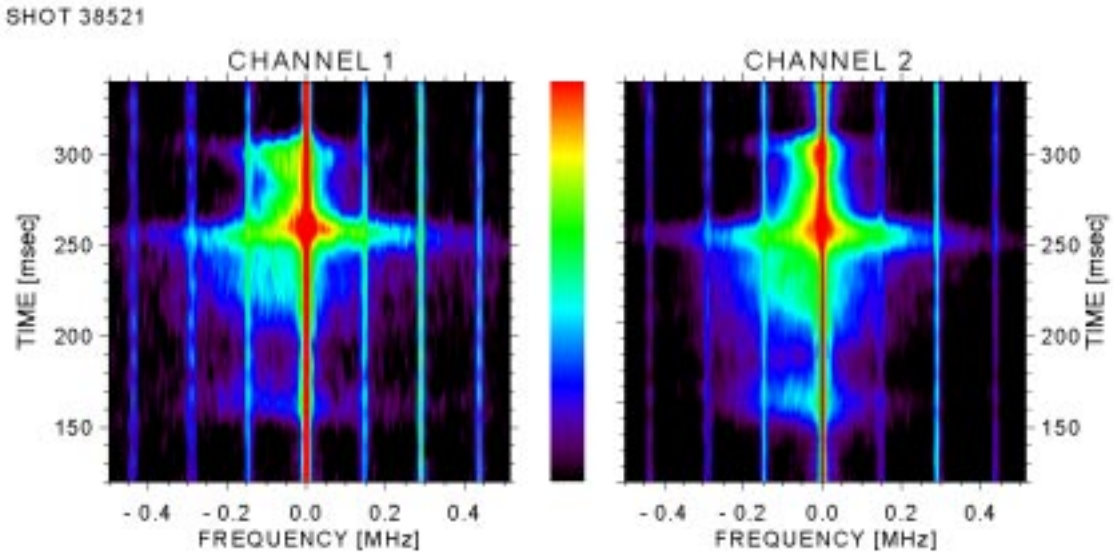

Figure 2. Transient burst in the turbulence intensity recorded under W7-AS shot 38521.

Initial measurements of plasma turbulence taken in early 1997 are shown in Figure 2. The figure gives a two-dimensional display of the temporal evolution of the power spectral density of the signals detected by the two detectors. The bright vertical line at zero frequency is due to local oscillator leakage, while the secondary vertical lines spaced by about 150 kHz are due to some background electrical interference. The turbulent burst lasts about 150 msec with the strongest fluctuations recorded at 255 msec after initiation of the plasma.

Figure 3 shows the spectral distribution at the peak of the burst. Comparison with the dotted line which corresponds to the start of the plasma pulse shows that the peak turbulence intensities are about 20 dB over the background noise level. These results are preliminary - ongoing work will aim at quantifying turbulence levels, and their spatial distribution, at W7-AS.

1. Association Euratom - Risø National Laboratory Annual Progress Report 1995.

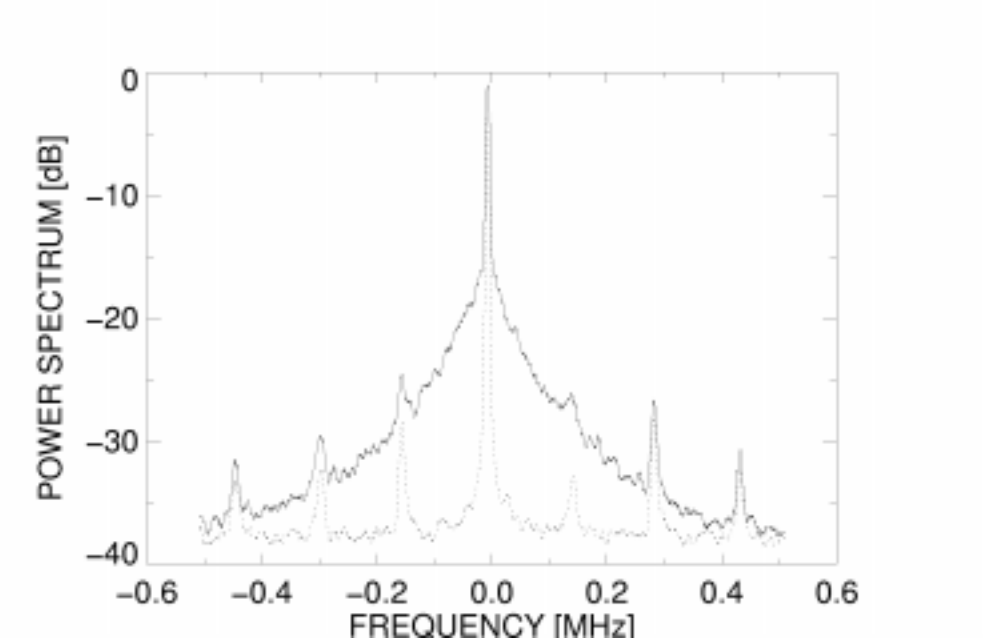

Figure 3. Power spectrum at 255 msec (solid line) and 0 msec (dotted line).

2.3 Nonlinear Dynamics of Fusion Plasmas

2.3.1 Localised Vortex Structures in Inviscid Plasma Flows

T. Jessen and P. K. Michelsen

A new highly efficient spectral computer code for two- and three-dimensional simulation has been developed. The main objective is to obtain a code for simulation of the response of a two-point collective scattering laser diagnostic to various types of plasma turbulence. As an initial test of the code the Euler equation was solved in a two-dimensional box using double periodic boundary conditions. Part of the verification procedure included the study of generation and breakdown of localised vortex structures. A variety of stable or long-lived structures has been observed. These include dipoles and also higher order poles, which have recently been observed in a number of experimental and numerical studies. Azimuthal perturbation of an initially radially shielded vortex is found to be a rich setting for generation of localised vortex structures. We perform the first systematic scan of parameter space, thereby outlining the basins of attraction of various vortex structures.

2.3.2 Resistive Coupling in Drift Wave Turbulence

P. K. Michelsen, T. Sunn Pedersen and J. Juul Rasmussen

Investigations of the two-dimensional Hasegawa and Wakatani model[1] for nonlinear plasma drift waves were continued with the main purpose

of getting an improved understanding of drift wave turbulence and the related cross-field particle transport. In this model the drift waves are linearly unstable and after a period of exponential growth, a nonlinear quasi-stationary turbulent state is achieved. The model equations were solved numerically in a two-dimensional domain of size $L_x \times L_y$. A reformulation of the model equations clearly brings out the effects of the coupling between the density and the electrostatic potential, due to the parallel electron coupling. The coupling can be reduced to a coupling constant if it is assumed that only one mode k_z exists in the parallel direction. The value chosen for the coupling coefficient C reflects a specific choice of the values of the parallel resistivity and the parallel wave number. The plasma turbulence was investigated for various values of the coupling coefficient.

In Figure 4a spectra of the total energy for various values of the coupling coefficient for a domain size of $L_x = L_y = 50$ are shown. It is seen that a maximum is obtained around $k = 1.0$ for small values of C and that the maximum occurs at lower $k-$values for larger values of C. The energy spectrum for $C = 10$ and $L_x = L_y = 150$ shown in Figure 4b was calculated to see the effect of the domain size. The statistics give some fluctuation in this spectrum; however, it seems clear that there is still a maximum that appears around $k = 0.2$.

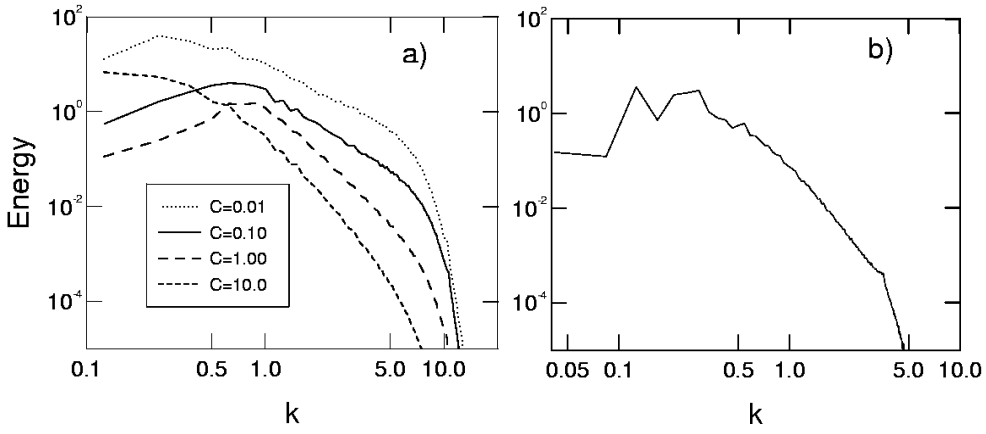

Figure 4: Spectra of total energy for various values of coupling coefficient and domain size. a) $L_x = L_y = 50$ and b) $L_x = L_y = 150$ and C = 10.

1. A. Hasegawa and M. Wakatani, *Phys. Rev. Letters* **50,** 682 (1983).

2.3.3 Contribution of Coherent Structures in Drift Wave Turbulence to Particle Transport

V. Naulin and K. H. Spatschek (Heinrich-Heine Universität, Düsseldorf, Germany)

Anomalous transport in magnetically confined plasmas is still not a phenomenon that is well understood. Basic processes have to be studied in reduced simple models. As drift waves are often made responsible for

transport in the scrape off layer (SOL), we here concentrate on the turbulent dynamics of drift waves and the coherent structures that emerge in the turbulent flow.

A one-field model for driven drift wave turbulence[1] that describes the universal and the drift dissipative instability is considered, and the equation is solved numerically.

The saturated turbulent state consists of random fluctuations and long-lived structures. The dynamics and properties of the latter coherent structures are of special interest. It is possible to identify coherent structures in the turbulent flow using the Weiss field.[2] Therefore, for the statistical evaluation of the motion of structures we search for all of them in each time step of the numerics and follow their movement over time. When monitoring structure displacements, however, we only consider events that last longer than an eddy turnover time. Using position vectors pointing to the structures, considering density humps/dips separately and, finally, weighting the contribution of each hump (or dip) by the corresponding trapped density, a mean position vector for maxima and minima, respectively, is defined.

The x- and y-coordinates of the structures that have thus been statistically averaged show that both maxima and minima move in the y-direction at the same (diamagnetic) velocity, whereas in the x-direction they move oppositely to each other (maxima down the density gradient; minima up the density gradient). As a result the structures are not dipole-like and do indeed account for transport as they move the particles trapped within them in the direction of the density gradient.

We are led to the following scenario for the particle transport: One contribution is the fluctuation induced transport which is due to a (slight) phase shift between density and potential fluctuations. The second component of the transport is caused by the movement of coherent structures in x-direction.

Estimates show that the coherent transport might become of the same order as the fluctuation induced component. However, we were able to derive an approximate relation between both kinds of transport; an approximation that states that the coherent flux should be a fraction δ of the fluctuation induced flux, with δ being a measure of the non-adiabaticity of the electron density response.

The numerical results shown in Figure 5 support this finding, but we should bear in mind that here we present only a rough estimate of the coherent transport as a more detailed theory for the dynamics of coherent structures in turbulent flows is still missing.

1. Volker Naulin, *Nichtlinearer Transport in ebenen Driftwellen-modellen*, PhD thesis, Heinrich-Heine Universität, Düsseldorf, 1995.
2. J. Weiss, *Physica D*, 48:273, 1991.

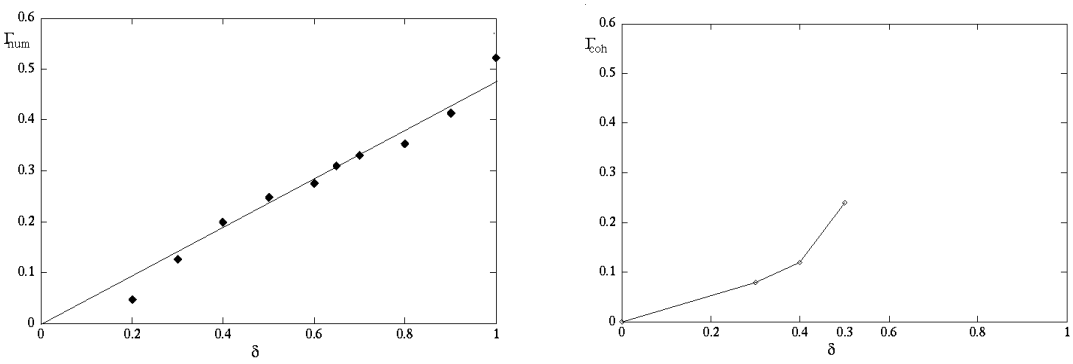

Figure 5. Fluctuation induced (left) and coherent (right) particle flux over deviation from adiabaticity δ. The fluctuation part shows ~δ behaviour, while the coherent transport is ~δ^2.

2.3.4 Extended Models of Flute- and Drift Modes in Plasmas Confined by Curved Magnetic Fields

K. Rypdal, O. E. Garcia (University of Tromsö, Norway), V. Naulin and J. Juul Rasmussen

Experimental observations from various magnetically confined plasmas show plasma turbulence that consists of large coherent structures immersed in a background of turbulence, which may well be of drift wave type. The flute structures are driven by the interchange instability, which is due to magnetic field curvature and a density gradient. The drift waves are driven unstable by density and/or temperature gradients in combination with a finite parallel resistivity. A model of the flute modes has been developed in [1], and a relevant model of the resistive drift waves is the well-known Hasegawa-Wakatani equations.[2] In the present work we develop a three-field model that contains both these models as special cases. In its most general form the model also allows for fluctuations in electron temperature in addition to plasma potential and electron density. By formulating this extended model the range of validity of the various reduced models can be investigated, and a proper reduction can more easily be found to describe a given experimental situation. A number of such reductions are under consideration.

1. K. Rypdal, H. Fredriksen, J. V. Paulsen and O. M. Olsen, *Physica Scripta* **T63**, 167-173 (1996).
2. A. Hasegawa and M. Wakatani, *Phys. Rev. Lett.* **50**, 682 (1983).

2.3.5 Detection of Coherent Plasma Structures: Verification of Experimental Methods by Application to Simulation Data

K. Rypdal, V. Naulin, P. K. Michelsen J. Juul Rasmussen, A. H. Nielsen and O. M. Olsen (University of Tromsö, Norway)

Observations from Q-machines and plasmas confined in simple toroidal geometries reveal plasma turbulence consisting of large coherent

structures immersed in a background of turbulence. Methods applied for detection of these structures include bispectral analysis of time series from a single probe,[1] and conditional averaging of time series data obtained from a fixed reference probe and a movable probe.[2] Improved understanding of the information obtained by these techniques can be gained by applying them to data where the full space-time information has been recorded. In plasma experiments such information would require a dense array of probes recording simultaneous time series, which is very difficult to achieve. However, in numerical simulations of models describing plasma turbulence such data can be recorded and it is possible to check for coherent structures using the Weiss field[3] and wavelet analysis.[4] In the present work the validity of existing detection methods will be put to a test by applying them to simulation data of drift wave turbulence as well as to simulation data of fluid turbulence. The latter will contribute to the understanding of the differences between these two types of turbulence.

1. K. Rypdal and F. Øynes, *Phys. Lett.* **A 184**, 114 (1993).
2. F. Øynes, H. L. Pécseli and K. Rypdal, *Phys. Rev. Lett.* **75**, 81 (1995).
3. J. Weiss, *Physica* **D 48**, 273 (1991).
4. Proceedings of the IEEE, Special Issue on Wavelets, April 1996.

2.3.6 Spiral Collapse and Turbulent Equilibrium of the Simple Magnetised Torus

K. Rypdal and O. E. Garcia (University of Tromsö, Norway)

The notion of a simple magnetised torus covers the plasma configurations where a plasma is confined by an axisymmetric toroidal magnetic field, without any poloidal field component. Although this configuration is known not to possess an MHD-equilibrium, it has proved to be very suitable for experimental investigation of waves, coherent structures, turbulence and anomalous transport. In fact, the configuration serves as a paradigm for those naturally occurring and man-made situations where plasmas are confined by curved magnetic fields, and where no rotational transform exists to prevent interchange instability. Experimental investigations have revealed the quasiperiodic occurrence of a large flute-like dipole vortex rotating poloidally with the flow of the bulk plasma. This vortex is found to be very active in mediating transport.

In the present work numerical simulations of a 2D fluid model show that the emergence of such a dipole structure could be the early stage of a driven collapsing spiral vortex. Just as in other more familiar wave collapse phenomena, the early stage of the collapse reflects a physical reality, but the later stage is the result of imperfections of the model. In our case such an imperfection is the assumption of flute-like perturbations. This is probably not a valid assumption when very large density gradients develop. Inclusion of resistive dynamics parallel to the magnetic field would drive drift waves and ion acoustic waves unstable, and would thereby open a channel for dissipation of energy that could lead to burnout of the spiral vortex. Such a burnout would pave the way

for a new vortex and, hence, a quasiperiodic occurrence of these structures.

The fluid equations are solved numerically in an entire poloidal cross-section and an example of the results is shown in Figure 6. The fluid equations are solved without many of the scaling assumptions and linearisations made in the standard models of drift waves and flute modes. Such models become invalid if the perturbations grow to a level where they strongly alter the background profile. In our model the free energy derives from explicit sources of plasma and electric charge, not from a fixed equilibrium profile. This corresponds closely to the experiments in question, which are steady state discharges produced by electron emission from a hot, negatively biased cathode.

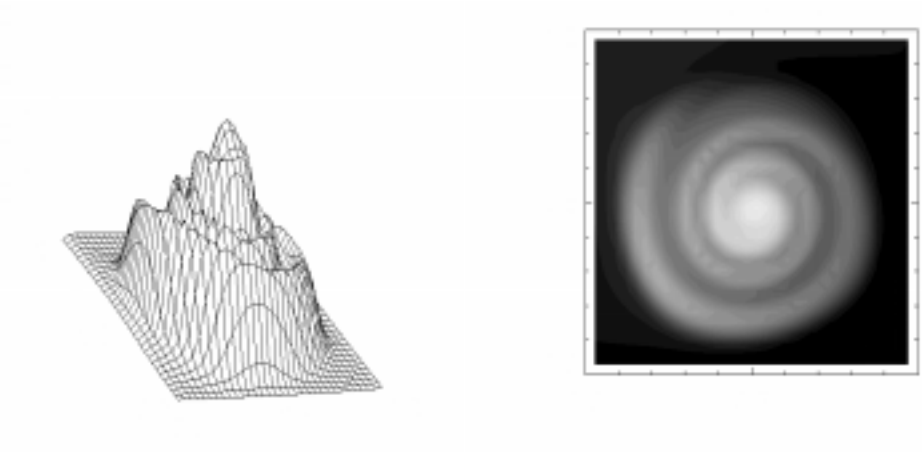

Figure 6. Simulation of fluid equations showing the electron density distribution (both as a three-dimensional and a contour plot) in a poloidal cross-section of a simple magnetised torus at a given time.

1. K. Rypdal, H. Fredriksen, J. V. Paulsen and O. M. Olsen, *Physica Scripta* **T63**, 167-173 (1996).

2.3.7 Two-dimensional Electron Magnetohydrodynamic Turbulence

N. Chakrabarti (Institute of Plasma Physics, Bhat, India),
P. K. Michelsen, J. Juul Rasmussen and K. Rypdal

Recently, special interest in electron magnetohydrodynamic turbulence has arisen to model collisionless reconnection that may be the origin of strong magnetic activity in nearly collisionless plasmas. Both two-dimensional high resolution and three-dimensional low resolution simulations have revealed that strong turbulence is excited by the current density gradients in the reconnection region, which gives rise to anomalous electron viscosity (see, e.g., [1]). In order further to study this turbulence together with vortex propagation and interaction, a model for the electron magnetohydrodynamics was investigated theoretically and numerically. The 2D model equations for the electron magnetohydrodynamics may be written in terms of two scalar quantities, the flux function ψ describing the magnetic field in the plasma

$\mathbf{B} = \hat{\mathbf{z}} \times \nabla \psi$ and a stream function b describing the poloidal electron flow $\mathbf{v} = \hat{\mathbf{z}} \times \nabla b$, which is proportional to the poloidal current density. The ions are assumed to be infinitely heavy so only the high frequency electron dynamics is considered. The evolution of stationary dipole solutions to the model equations is investigated.

1. D. Biskamp, E. Schwarz and J. F. Drake, *Phys. Rev. Letters* **76,** 1264 (1996).

2.3.8 Shear Flow Effect on Ion Temperature Gradient Vortices in Plasmas with Sheared Magnetic Field

N. Chakrabarti (Institute of Plasma Physics, Bhat, India),
J. Juul Rasmussen and P. K. Michelsen

The effect of velocity shear on ion temperature gradient (ITG) driven vortices in a nonuniform plasma in a curved, sheared magnetic field is investigated. In absence of parallel ion dynamics the toroidal branch of the ITG mode vortices is studied analytically assuming a Gaussian equilibrium profile of the density. It has been shown that the coupled potential and pressure equations exhibit solutions in the form of tripolar vortex-like structures. These structures are special cases and arise at resonance (when the flow velocity matches the velocity of the propagating vortex). For the general case, however, we include parallel ion dynamics, and the equation describing the stationary ITG vortex has the structure of a nonlinear Poisson-like equation. For a simplified case, the analytic solution indicates the existence of a monopolar vortex structure away from the velocity shear layer. The most general solution is solved numerically. It is shown that, for a critical value of the velocity shear, asymmetric dipolar vortices can arise. At resonance these vortex structures are strongly modified and a localised vortex chain may be formed. For large velocity shear these structures are destroyed and ultimately lead to a shear driven structure with a dominating monopolar part. The effect of magnetic shear on velocity shear induced vortices is also studied. Qualitative results indicate that magnetic shear destroys these structures in the sense that no localised stationary solutions seem to exist when the magnetic shear strength exceeds a (low) threshold value.

Preliminary investigations of the dynamic evolution and stability of the velocity shear vortex structure by numerically solving the evolution equations indicate that they are unstable, at least for the strong shear cases.

2.3.9 Vortex Merging and Corresponding Energy Cascade in Two-dimensional Electrostatic Turbulence

A. H. Nielsen, J. Juul Rasmussen and M. R. Schmidt

For two-dimensional electrostatic turbulence it is well established that the energy is cascading towards larger scales resulting in the build-up of large-scale structures. This inverse cascade is believed to be mediated by merging of like-signed vortices. The enstrophy (mean squared vorticity - equivalent to the mean squared charge density in electrostatic

turbulence), on the other hand, cascades directly towards smaller scales. To provide detailed understanding of this cascading process we have investigated the simple case of the merging of two equally signed monopoles with Gaussian distributed charge density by numerically solving the Euler equations by a high resolution double-periodic spectral code.

The temporal evolution of the charge density together with the Weiss field, $s = ¼(\sigma^2-\omega^2)$, is shown in Figure 7. During the merging process spiral filaments in the charge density are created. These filaments are stretched infinitely in the straining field resulting from closer interaction of the monopoles. From the Weiss field we see that the cores of the monopoles are rotation-dominated, $s < 0$, whereas just outside the monopoles a strong straining field is present, $s > 0$. Our simulations also identify that the enstrophy cascade is most active on the disordered vortex boundaries and to a certain degree also in the filaments, with a localised energy spectrum, $E(k) \approx k^{-4}$, developed at high wave numbers. A similar spectrum will be obtained if, instead of only two like-signed monopoles, we were initialising a large number of monopoles with different sizes and polarities.

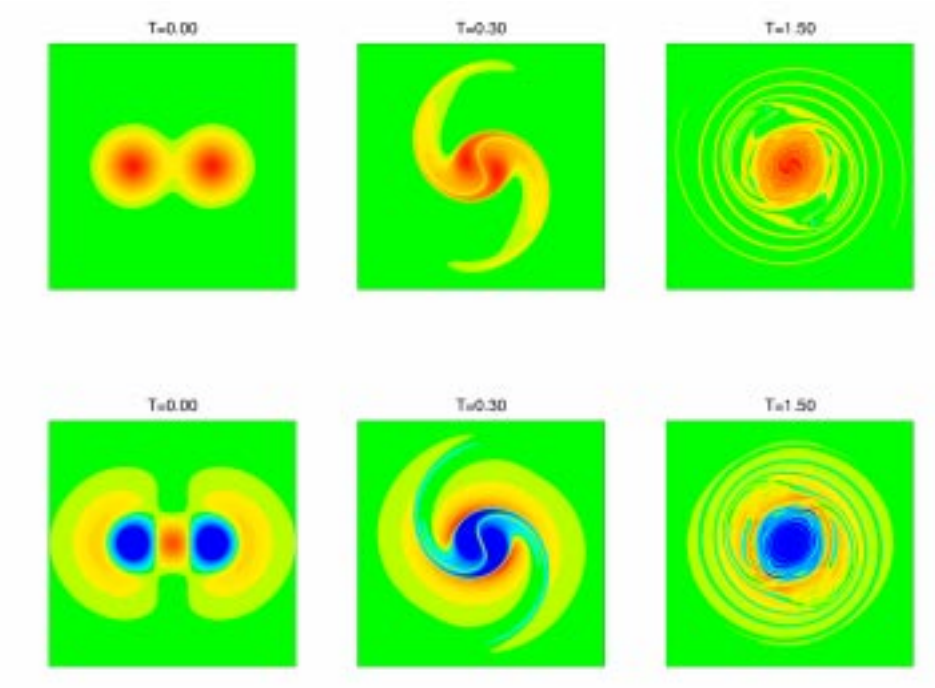

Figure 7. Computer simulation of the merging of two identical monopoles with Gaussian distributed charge density. The first row displays the temporal evolution of the vorticity while the second row displays the corresponding Weiss field, $s = ¼(\sigma^2-\omega^2)$. Full lines are for positive values; dashed lines are for negative values. A resolution of 1024 x 1024 and a sixth-order hyper viscosity with $\mu = 10^{-18}$ were used.

2.3.10 Particle Tracking in a Two-dimensional Flow Field

A. H. Nielsen and J.P. Lynov

Particle tracking in plasma and fluid dynamics is an important tool for determining the transport properties of a flow field. Generally, we solve the plasma fluid equations in the guiding centre approximation (equivalent to the Navier-Stokes equations) in the Eulerian framework where the flow field is known at all times in a (fixed) spatial grid. The fluid inside a small fluid element located at a grid point will consist of different fluid particles at different times. The information about how these particles are transported or convected by the flow field is not directly present in this framework.

We have solved the plasma fluid equations numerically using highly accurate spectral methods. The domain could either be double-periodic or an annulus with one bounded direction and one periodic. For the periodic directions we use Fourier modes as expanding functions, whereas for the bounded direction we use Chebyshev polynomials. To follow the trajectories of the fluid particles we evaluate the full spectral expansion of the velocity field. Thereby we use all the information stored in the flow field. Such evaluations are quite expensive in terms of computer time, and 200-300 particles take as much CPU time as solving the fluid equations alone. We have therefore implemented the computer code on an SP2 parallel supercomputer located at UNI*C, Lyngby, Denmark.

An example of our particle simulation is shown in Figure 8. Here the cross field particle motion out of coherent structures, in which the particles are trapped originally, is shown. The untrapping of the particles is due to the plasma being in a parameter regime with slightly unsteady flow properties.

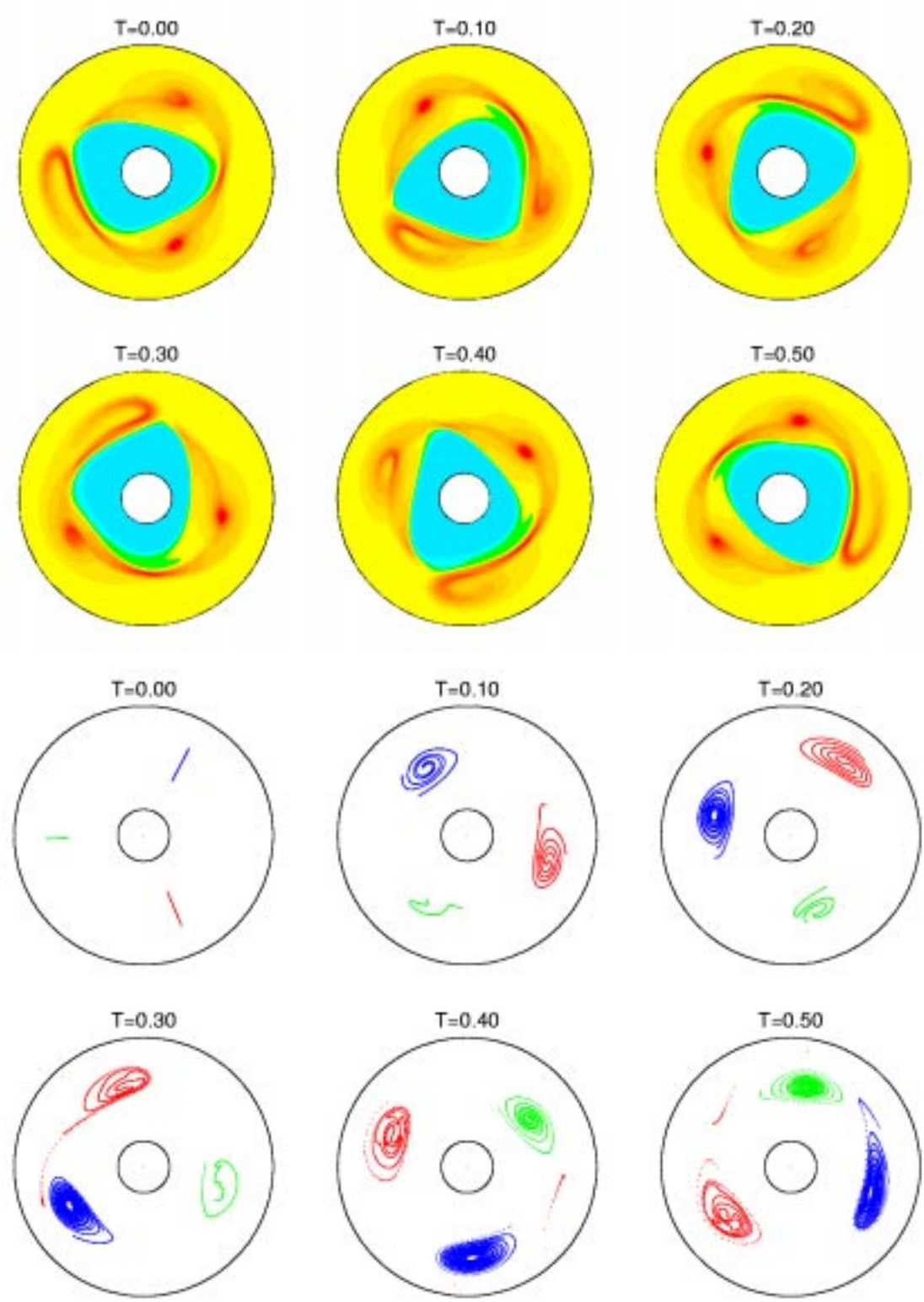

Figure 8. Upper part: Time evolution of the charge density in a forced annular shear flow where an unstable mode 3 is perturbed by a counter clock-wise rotating mode 1. Lower part: Corresponding particle simulation where 6.000 passive particles are traced with spectral accuracy using the velocity field calculated from the charge density shown in the upper part of the figure. The spectral resolution is 256 Chebyshev modes and 256 Fourier modes and the equivalent Reynolds number 403.

2.3.11 Self-focusing of Electromagnetic Waves in a Magnetised Plasma

M. R. Schmidt and J. Juul Rasmussen

The slowly varying amplitude field of high frequency electromagnetic waves propagating in a magnetised plasma is modelled by the generalised three-dimensional cubic Schrödinger equation:

$$i\frac{\partial\psi}{\partial t}+\nabla_\perp^2\psi+s\frac{\partial^2\psi}{\partial z^2}+p|\psi|^2\psi=0\ ,\ \text{where}\ \nabla_\perp^2\psi\equiv\frac{\partial^2\psi}{\partial x^2}+\frac{\partial^2\psi}{\partial y^2}$$

ψ is the complex scalar envelope field and z is the direction of the propagation, which is the in the direction of the magnetic field. The second term models the diffraction in the transverse plane; the third term models the dispersion along the axis of propagation (s > 0 yields anomalous dispersion, s < 0 yields normal dispersion). The last term on the left-hand side describes the non-linear refractive index depending on the intensity of the electromagnetic waves, where p > 0 corresponds to focusing, and p < 0 corresponds to defocusing. As the equation is nondimensionalised, only the signs of s and p are important, giving four regimes with different dynamics. Most previous studies were based on the assumption of isotropic dispersion relationships of the plasma (s > 0), or radial symmetry in the solution.

To study the complete three-dimensional dynamics of electromagnetic wave fields, we have implemented a pure spectral code that solves the cubic Schrödinger equation in a triple periodic geometry with time integration performed by a third-order Adam-Moulton predictor-corrector scheme with fixed time step. We have also studied a split-step and a stiffly stable time integration instead of the Adam-Moulton scheme. Especially the split-step scheme is appropriate for the cubic Schrödinger equation, as it conserves the invariants, and change of time step is possible without loss of accuracy and computational time.

We have conducted preliminary investigations of the internal dynamics of electromagnetic wave beams in idealised, homogeneous media. An interesting phenomenon in anisotropic media with s < 0 is the competing mechanisms of splitting in the *z*-direction (the direction of propagation) and self-contraction in the transverse plane, for p > 0. It is well established that self-focusing in two and three dimensions in media with s > 0 can lead to a so-called “collapse” or “blow-up”, where the field becomes singular. This takes place in finite time, provided that the beam intensity exceeds some critical value inside an effectively bounded area. It is also quite well established that for s < 0 beams focusing in two dimensions will split along z into smaller structures, which can successively undergo further splitting. The splitting process stops when the intensity of the involved structures decreases below a critical value. Preliminary results indicate that splitting takes place before the field (a spherical Gaussian field distribution) can collapse. However, a more detailed study is necessary to validate the observation.

2.3.12 Amalgamation of Interacting Electromagnetic Wave Beamlets in Plasmas

L. Bergé (CEA/Limeil-Valenton, Villeneuve-Saint-Georges cedex, France), M. R. Schmidt, J. Juul Rasmussen, P. L. Christiansen and K. Ø Rasmussen* (* IMM, The Technical University of Denmark, Lyngby, Denmark)*

Self-trapping and self-focusing of intense electromagnetic wave beams propagating in magnetised as well as unmagnetised plasmas have been widely investigated since the 1960s. In particular, self-trapped beams evolving in three spatial dimensions (3D) are well-known to be unstable within an ideal plasma with cubic nonlinearity and to break up into a train of 3D solitary waves. In the absence of saturation, the resulting filaments self-focus until they collapse at a finite propagation distance, when their individual power is such that the non-linear effects continuously dominate over the natural dispersion of the wave. In this regime, the "energy" - or Hamiltonian - integral associated with the filaments is negative and the transverse power of the input beam must exceed a critical threshold. These results apply to individual electromagnetic beams. Often a number of filaments are formed as a result of the modulational instability of a broad electromagnetic beam. These filaments are observed to interact, but up to now no quantitative investigation of this interaction dynamics has been performed.

The aim of our work is to contribute to the theory of interacting electromagnetic beams by considering the possible interaction regimes for two filaments in a plasma with a self-focusing cubic nonlinearity. The nature of the interaction is shown to vary with the incident individual powers and relative phases of the beamlets. By means of virial arguments supported by numerical results it is found that three distinct evolution regimes characterise two in-phase interacting filaments: (i) When each of the filaments has a power below $N_c/4$, where N_c is the critical self-focusing threshold for a single beam, they both disperse along their propagation axes. (ii) When their respective powers lie between $N_c/4$ and N_c, they fuse into a single central lobe which may self-focus until collapse, depending on the initial separation distance; this distance below which the central lobe forms and can collapse is estimated analytically. An example of this behaviour is shown in Figure 9. (Here $N_c = 4\pi$.) (iii) When their incident powers both exceed N_c, initially separated filaments individually self-focus without mutual interaction. In contrast to in-phase beamlets, two beamlets with opposite phase are shown never to coalesce.

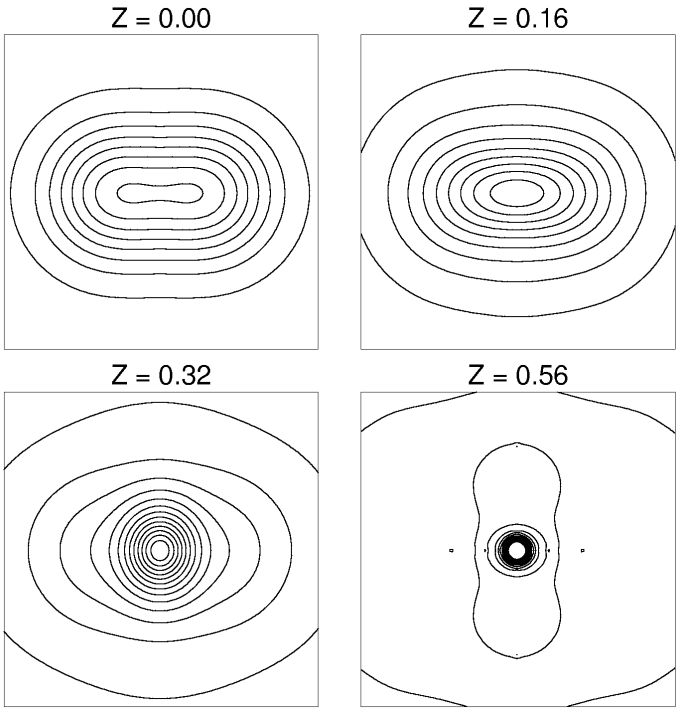

Figure 9. Contour plots for the amplitude field of two interacting beamlets. Each beamlet has a power of 2π; isolated they would spread out. Together, however, the total power of the two beamlets, including the interaction between them, exceeds 4π. This causes them to fuse into one central lobe and collapse at the propagation distance $z = 0.58$.

2.4 External Projects

2.4.1 Pellet Injectors

P.K. Michelsen, B. Sass, and J. Bundgaard (Engineering and Computer Department)

After the delivery of two eight-shot hydrogen/deuterium pellet injectors to ENEA (FTU and RFX) further research and development in this area has been terminated. However, some technical support to the groups with Risø-made pellet injectors is continued. B. Sass has visited FOM in order to assist with a minor change and adjustment of the RTP pellet injector. Advice has been given to both the FTU and the RFX pellet groups with respect to the electronic control system of the pellet injectors and with respect to the possibility of combining the Italian two-stage injector with the multishot Risø-injector.

2.4.2 Remote Wind Measurements for Control of Windmills

L. Lading and M. Saffman

As a spin-off from the work on plasma turbulence measurements by collective light scattering, a method for remote measurement of wind velocity for feed forward control of wind turbines has been devised and a patent application submitted. The work is being performed in collaboration with two industrial companies. One is a major manufacturer of large wind turbines and the other commercial partner is an engineering company designing wind turbines and automation equipment. Initiatives have been taken to establish an industrial European collaboration. The technological basis for the work has a considerable overlap with the laser diagnostics being developed for measurements at the W7-AS stellarator at IPP Garching.

2.4.3 Fusion EXPO Exhibition in Denmark

V.O. Jensen

The exhibition "FUSION EXPO: Harnessing the energy of the sun" was opened on August 16th 1996 at the Elmuseum (Electricity Museum) in Bjerringbro, Jutland, by the Danish minister for Research and Information Technology, Mr. Frank Jensen. In his opening speech Mr. Jensen mentioned that the Danish Government considered fusion energy as an interesting option for the energy supply of mankind in the future.

In discussions after the official opening, Mr. Frank Jensen suggested that the Elmuseum could act as an information centre for high school students and teachers concerning new trends in science and technology. As a result, it is now planned to arrange a two days seminar on fusion in 1998 where some 30 teachers will learn about fusion research and its promises.

During the 6 weeks the exhibition was on display in Denmark, a total of some 9000 visitors saw the FUSION EXPO and out of this some 40 high school classes had asked for and got special guided tours.

2.5 Participants in Fusion Plasma Physics

Scientific Staff

Jensen, Vagn O.	
Junker, Wolfgang	(until 30 April)
Lading, Lars	(part time ~10%)
Lynov, Jens-Peter	
Michelsen, Poul K.	
Nielsen, Anders H.	
Rasmussen, Jens Juul	
Saffman, Mark	

Post Docs

Naulin, Volker	(from 1 September)

Svendsen, Winnie E. (from 1 May)

Ph.D. Students

Jessen, Thomas
Schmidt, Michel R.

Technical Staff

Astradsson, Lone	
Bækmark, Lars	
Jensen, Monika	(part time ~10%)
Reher, Børge	(part time ~60%)
Sass, Bjarne	(part time ~50%)
Thorsen, Jess	

Guest Scientists

Chakrabarti, Nikhil, Institute of Plasma Research, Bhat, India
Hesthaven, Jan, Brown University, Rhode Island, USA
Rypdal, Kristoffer, University of Tromsø, Norway
Saeki, Koichi, Shizuoka University, Japan

Short-term Visitors

Bergé, Luc, Commissariat á l'Energie Atomique, Centre d'Etudes de Limeil-Valenton, France
Grauer, Rainer, Heinrich-Heine-Universität, Düsseldorf, Germany
Karpman, Vladimir I., Racah Institute of Physics, Hebrew University, Jerusalem, Israel
Kuznetsov, Evgenii A., Landau Institute, Moscow, Russia
Pécseli, H.L., University of Oslo, Norway
Wyller, John, Narvik Institute of Technology, Norway
Yankov, V.V., Russian Research Center Kurchatov Institute, Moscow, Russia
Zakharov, V.E., Landau Institute, Moscow, Russia

2.6 Publications and Educational Activities

2.6.1 Publications

Bergé, L.; Kuznetsov, E.A.; Rasmussen, J. Juul, Defocusing regimes of nonlinear waves in media with negative dispersion. Phys. Rev. E (1996) v. 53 pp R1340-R1343.

Bergé, L.; Kuznetsov, E.A.; Rasmussen, J. Juul; Shapiro, E.G.; Turitsyn, S.K., Self-focusing of optical pulses in media with normal dispersion. Phys. Scr. (1996) v. T67 pp 17-20.

Bergé, L.; Rasmussen, J. Juul, Multisplitting and collapse of self-focusing anisotropic beams in normal/anomalous dispersive media. Phys. Plasmas (1996) v. 3 pp 824-843.

Bergé, L.; Rasmussen, J. Juul; Kuznetsov, E.A.; Shapiro, E.G.; Turitsyn, S.K., Self-focusing of chirped optical pulses in media with normal dispersion. J. Opt. Soc. Am. B (1996) v. 13 pp 1879-1891.

Bergeron, K.; Coutsias, E.A.; Lynov, J.P.; Nielsen, A.H., Self-organization in circular shear layers. Phys. Scr. (1996) v. T67 pp 33-37.

Coutsias, E.A.; Hagstrom, T.; Hesthaven, J.S.; Torres, D., Integration preconditioners for differential operators in spectral *tau*-methods. In: ICOSAHOM-95. Proceedings. 3. International conference on spectral and high order methods, Houston, TX (US), 5-9 Jun 1995. Ilin, A.V.; Ridgway Scott, L. (eds.), (Houston Journal of Mathematics, Houston, TX, 1996) (Houston Journal of Mathematics) pp 21-38.

Coutsias, E.A.; Hesthaven, J.S.; Lynov, J.P., New spectral algorithms for accurate simulations of bounded flows. In: Advanced concepts and techniques in thermal modelling. Eurotherm seminar 36, Poitiers (FR), 21-23 Sep 1994. Lemonnier, D.; Saulnier, J.B.; Fiebig, M. (eds.), (Elsevier, Amsterdam, 1996) pp 119-127.

Jensen, V.O., Fusionsenergien: Kommer den, og hvad kommer den til at betyde?. EL og Energi (1996) v. 92 (no.9) pp 34-35.

Karpman, V.I.; Lynov, J.P.; Michelsen, P.K.; Rasmussen, J.J., Modulational instability of plasma waves in two dimensions. Math. Comput. Simul. (1996) v. 40 pp 223-234.

Lading, L.; Saffman, M.; Hanson, S.G.; Edwards, R.V., A combined doppler and time-of-flight laser anemometer for measurement of density fluctuations in plasmas. J. Atmos. Terr. Phys. (1996) v. 58 pp 1013-1019.

Lynov, J.P.; Singh, B.N. (eds.), Association Euratom - Risø National Laboratory annual progress report 1995. Risø-R-897(EN) (1996) 70 p.

Nielsen, A.H.; He, X.; Rasmussen, J. Juul; Bohr, T., Vortex merging and spectral cascade in two-dimensional flows. Phys. Fluids (1996) v. 8 pp 2263-2265.

Nielsen, A.H.; Pécseli, H.L.; Rasmussen, J.J., Turbulent transport in low-beta plasmas. Phys. Plasmas (1996) v. 3 pp 1530-1544.

Nielsen, A.H.; Rasmussen, J. Juul; Schmidt, M.R., Self-organization and coherent structures in plasmas and fluids. Phys. Scr. (1996) v. T63 pp 49-58.

Hanson, S.G.; Lading, L.; Lynov, J.P.; Skaarup, B. (eds.), Optics and Fluid Dynamics Department annual progress report for 1995. Risø-R-865(EN) (1996) 90 p.

Pedersen, T.S.; Michelsen, P.K.; Rasmussen, J.J., Lyapunov exponents and particle dispersion in drift wave turbulence. Phys. Plasmas (1996) v. 3 pp 2939-2950.

Pedersen, T.S.; Michelsen, P.K.; Rasmussen, J. Juul, Resistive coupling in drift wave turbulence. Plasma Phys. Control. Fusion (1996) v. 38 pp 2143-2154.
Pedersen, T.S.; Michelsen, P.K.; Rasmussen, J. Juul, Analysis of chaos in plasma turbulence. Phys. Scr. (1996) v. T67 p 30-32.
Rasmussen, J.J.; Hesthaven, J.S.; Lynov, J.P.; Nielsen, A.H.; Schmidt, M.R., Dipolar vortices in two-dimensional flows. Math. Comput. Simul. (1996) v. 40 pp 207-221.
Tachon, J.; Lawson, J.; Jensen, M.I.; Jensen, V.O. (eds.), Fusion expo. Energi fra solens egen energikilde. (Europa-Kommissionen. DG XII. Europæiske Fusionsprogram, Bruxelles, 1996) 43 p.

2.6.2 Unpublished Contributions

Bergé, L.; Juul Rasmussen, J.; Schmidt, M.R., Amalgamation of interacting light beams in Kerr-type media. Annual meeting of the Danish Optical Society, Risø (DK), 21-22 Nov 1996. Unpublished. Abstract available.
Jensen, V.O., EU's fusionsprogram set ud fra et forskningssynspunkt. Møde om EU's fusionsprogram, incl. ITER. Forskningsministeriet, København (DK), 26 Feb 1996. Unpublished.
Jensen, V.O., Fusionsforskning. Kursus for fysiklærere fra 'Kursusregion Syd', Risø (DK), 15 Mar 1996. Unpublished.
Jensen, V.O., Fusion energy - the solution of the future. Seminar for project Lycée Carriat and Herlev Gymnasium, Risø (DK), 11 Apr 1996. Unpublished.
Jensen, V.O., Fusion. Seminar for lærere fra Hässleholm Tekniska Skole, Risø (DK), 2 May 1996. Unpublished.
Jensen, V.O., Fusionsenergi i fortid, nutid og fremtid. Fusion expo - solens kraftværk til jordens folk. Åbningsceremoni. Elmuseet, Bjerringbro (DK), 16 Aug 1996. Unpublished. Abstract available.
Jensen, V.O., Fusion work at Risø, future plans. Fusion Expo Consortium meeting. Centre de Recherches en Physique des Plasmas, Lausanne (CH), 23-24 Oct 1996. Unpublished.
Jensen, V.O., Plasma Physics, 28 lectures at the Danish Technical University, 1996. Unpublished.
Junker, W.; Saffman, M.; Lading, L., Spatially resolved measurements of density fluctuations with a hybrid doppler/time-of-flight laser anemometer. In: 1996 CLEO/Europe. Technical digest. Conference on lasers and electro-optics Europe, Hamburg (DE), 8-13 Sep 1996. (IEEE, Piscataway, NJ, 1996) p. 151.
Lynov, J.-P., Experimental and numerical studies of coherent structures in fluids and plasmas. ERCOFTAC Nordic pilot center meeting, Stockholm (SE), 5-6 Sep 1996. Unpublished.
Michelsen, P.K., Numerical studies of drift wave turbulence. Joint Varenna - Lausanne international workshop on theory of fusion plasmas, Varenna (IT), 26-30 Aug 1996. Unpublished.
Michelsen, P.K.; Juul Rasmussen, J., Vortex dynamics in low-frequency electrostatic turbulence. 5. Symposium on double layers - potential

formation and related nonlinear phenomena in plasmas. Tohoku University, Sendai (JP), 17-19 Sep 1996. Unpublished. Abstract available.

Michelsen, P.K.; Sunn Pedersen, T.; Juul Rasmussen, J., Lyapunov exponents and particle dispersion in drift-wave turbulence. 1996 International conference on plasma physics, Nagoya (JP), 9-13 Sep 1996. Unpublished. Abstract available.

Michelsen, P.K.; Sunn Pedersen, T.; Juul Rasmussen, J., Resistive coupling in drift wave plasma turbulence. 1996 International conference on plasma physics, Nagoya (JP), 9-13 Sep 1996. Unpublished. Abstract available.

Naulin, V., Vortex structures and transport in drift-wave turbulence. Düsseldorf University, Düsseldorf (DE), 19 Dec 1996. Unpublished.

Naulin, V., Structures in drift-wave turbulence and their impact on particle transport. Joint Varenna-Lausanne International workshop on Theory of Fusion Plasma, Varenne, Italy, 26-30 August 1996.

Naulin, V., Contribution of coherent structures to particle transport in driftwave turbulence. Euroconference on Supercomputation in Nonlinear and Disordered Systems: Algorithms, Applications and Architectures San Lorenzo de El Escorial, Marid, Spain, 23-28 September 1996.

Nielsen, A.H.; Rasmussen, J. Juul, Trapped passive particles in two-dimensional coherent structures. 21. General assembly of the European Geophysical Society, The Hague (NL), 6-10 May 1996. Ann. Geophys. Suppl. 2 (1996) v. 14 p. C612

Nielsen, A.H.; Rasmussen, J.J.; He, X., Trapped passive particles in two-dimensional coherent structures. Annual meeting of the Danish Physical Society, Nyborg (DK), 23-24 May 1996. Unpublished. Abstract available.

Rasmussen, J. Juul, Electron beam instabilities in plasmas. Royal Institute of Technology. Alfvén Laboratory, Stockholm (SE), 2 Feb 1996. Unpublished.

Rasmussen, J. Juul, Self-organization and coherent vortical structures in plasmas, fluids and optics. Seminar Ionenphysik. Universität Innsbruck. Institut für Ionenphysik, Innsbruck (AT), 4 Jun 1996. Unpublished.

Rasmussen, J. Juul, Transport and turbulence in a low-beta plasma. Seminar Energie- und Plasmaphysik. Universität Innsbruck. Institut für Ionenphysik, Innsbruck (AT), 5 Jun 1996. Unpublished.

Rasmussen, J. Juul, Turbulence and transport in fluids and plasmas. EPS 10. Trends in physics. 10. General conference of the European Physical Society, Sevilla (ES), 9-13 Sep 1996. Unpublished. Abstract available.

Rasmussen, J. Juul, Vortex merging and spectral cascade in two-dimensional flows. Isaac Newton Institute for Mathematical Sciences. University of Cambridge, Cambridge (GB), 21 Oct - 1 Nov 1996. Unpublished.

Schmidt, M.R.; Rasmussen, J. Juul; Nielsen, A.H., Inverse cascade and intermittency in 2D turbulence. 21. General assembly of the European

Geophysical Society, The Hague (NL), 6-10 May 1996. Ann. Geophys. Suppl. 2 (1996) v. 14 p. C676.

Schmidt, M.R.; Rasmussen, J.J.; Nielsen, A.H., Inverse cascade and intermittency in 2D turbulence. Annual meeting of the Danish Physical Society, Nyborg (DK), 23-24 May 1996. Unpublished. Abstract available.

3. Fusion Technology

3.1 Introduction

The work reported in this section has been carried out in the Materials Department. The overall objective of the research activities in this area is to determine the impact of neutron irradiation on physical and mechanical properties of metals and alloys, so that appropriate materials can be chosen for their application in an irradiation environment (e.g. in a fusion reactor). Various experimental techniques are employed to study different aspects of the microstructural evolution during irradiation and the resulting consequences on the post-irradiation physical and mechanical properties of metals and alloys. Computer simulation are carried out to understand the evolution of surviving defects and their clusters in collision cascades. The kinetics of defect accumulation during irradiation and the influence of irradiation-induced defects and their clusters on the deformation behaviour of irradiated metals and alloys are studied theoretically. In the following, the main results of these activities are highlighted.

3.2 Next Step Technology (ITER Task T213/EU)

3.2.1 Effects of Pre-irradiation Heat Treatments and Irradiation on Microstructure and Physical and Mechanical Properties of Copper and Copper Alloys

B.N. Singh, D.J. Edwards, M. Eldrup, and P. Toft (*Pacific Northwest National Laboratory, USA)*

Low dose screening experiments were initiated on all three of the candidate copper alloys (i.e. CuAl-25, CuCrZr and CuNiBe) for ITER. The goal of the experiments was two-fold: first, to help understand what effect the joining treatment might have on the performance of these alloys after irradiation at various temperatures, and secondly, to narrow the number of alloys to two alloys, one main alloy and its backup. A series of heat treatments were given to CuCrZr, CuNiBe and CuAl-25 to simulate the effect of possible joining treatments such as hot isostatic pressing. The results of the first set of experiments on these alloys on the effect of various heat treatments on the mechanical properties, electrical resistivity and microstructure both before and after irradiation at 250^{o}C (to 0.3 dpa) were reported last year.

The present report summarises the results of a second set of experiments on the same materials irradiated to the same dose of 0.3 dpa,

but at 350°C instead. The effect of the various heat treatments described herein on the unirradiated microstructure have already been reported and will not be presented in this report in detail. Tensile properties of unirradiated and irradiated specimens with various heat treatments tested at 350°C are described. The results of electrical resistivity measurements at 23°C are also presented. The effect of irradiation on the microstructure of the various alloys is illustrated.

The materials used in the present investigations were CuCrZr, CuNiBe and CuAl-25 alloys. The CuCrZr and CuNiBe alloys were supplied by Tréfimétaux (France) in the form of 20 mm thick plates. In addition, Hycon 3HP™ (heat number 33667), a CuNiBe alloy produced by Brush Wellman Inc. (USA), was also included in this experiment. The ODS copper alloy Glid Cop™ CuAl-25 was supplied by OGM Americas (formerly SCM Metals Inc.) in the form of rods in the as-extruded (i.e. wrought) condition.

Flat tensile specimens (gauge length = 7.0 mm) were cut from cold-rolled (~80%) sheets (0.3 mm thick) of the Tréfimétaux CuCrZr and CuNiBe alloys, and from the as-received block of Hycon 3HP™. Round tensile specimens of CuAl-25 (of gauge diameter 3 mm) were machined from the as-supplied rod, which was in the as-wrought condition (i.e. no additional cold-work after extrusion).

TYPE	HEAT TREATMENT
Hycon	Proprietary, but essentially solution annealed, quenched, cold worked, and aged to produce an HT temper condition
A	Solution annealing at 950°C for 1 h followed by water quench
E	Prime ageing: heat treatment A + ageing at 475°C for 30 min. followed by water quench
B	Bonding thermal cycle: heat treatments A + E + annealing at 950°C for 30 min. followed by furnace cooling + re-ageing at 475°C for 30 min. followed by furnace cooling
C	Bakeout thermal cycle: heat treatment B + annealing at 350°C for 100 h followed by furnace cooling
C´	Bakeout thermal cycle: heat treatment E + annealing at 350°C for 100 h followed by furnace cooling
D	Annealing at 950°C for 30 min. (only for CuAl-25)
D´	CuAl-25 in the as-wrought condition, i.e. without any heat treatment

Table 1. Summary of bonding and bakeout heat treatments for CuCrZr, CuNiBe and CuAl-25 alloys.

For the screening experiments, the tensile specimens of Tréfimétaux CuCrZr and CuNiBe were given the five different heat treatments (A, B, E, C and C´) listed in Table 1. The bonding thermal heat treatment for CuAl-25 specimens consisted of annealing at 950°C for 30 min. (referred to as heat treatment D). The bakeout treatment was not given to the CuAl-25 since it is well known that this temperature has little effect on microstructure and properties of the alloy. All heat treatments were carried out in vacuum ($<10^{-5}$ torr). The details of the proprietary heat

treatment of the Hycon alloy are not known, but the alloy is essentially in a fully hardened condition (HT temper designation). It was irradiated in the as-received condition.

Tensile specimens of CuCrZr, CuNiBe, Hycon, and CuAl-25 alloys with the different heat treatments were irradiated at 350^{o}C in the DR-3 reactor at Risø in the High Temperature Rig. All specimens were irradiated at the same time to a fluence level of 1.5 x 10^{24} n/m^2 (E > 1 MeV), which corresponds to a displacement dose level of ~0.3 dpa (NRT). The neutron flux during irradiation was approximately 2.5 x 10^{17} n/m^{2}s (E > 1 MeV) which corresponds to a displacement damage rate of ~5 x 10^{-8} dpa (NRT)/s. Both unirradiated and irradiated tensile specimens (2 specimens from each condition) were tested in an Instron machine at a strain rate of 1.2 x 10^{-3} s^{-1}. Tensile tests were carried out at 350^{o}C in vacuum (<10^{-4} torr). The test temperature of 350^{o}C was reached within 30 minutes. The cross-head displacement was measured and used to determine the stress-strain behaviour of the specimens. For transmission electron microscopy (TEM) investigations, 3 mm discs from the unirradiated and irradiated specimens were electropolished and examined in a JEOL 2000 FX transmission electron microscope. The fracture surfaces of the irradiated as well as unirradiated specimens were examined in a JEOL 840 scanning electron microscope.

The electrical resistivity measurements were made at 23^{o}C on the unirradiated reference tensile specimens of OFHC-Cu, CuCrZr, CuNiBe and CuAl-25 with different heat treatments. The post irradiation resistivity was also measured at 23^{o}C. All resistivity measurements were made using one of the modules in the A 1931a Temperature Controller developed by the Electronics Department at Risø.

The heat treatment B corresponding to the bonding thermal cycle and re-ageing led to three main effects in CuNiBe: (a) formation of the precipitate denuded zone along grain boundaries, (b) formation of relatively large precipitates at grain boundaries, and (c) coarsening of small coherent precipitates (Table 2) in the matrix. None of these effects were observed in CuCrZr specimens after heat treatment B.

The most pronounced effect of irradiation on the microsctructural changes was observed in the solution annealed (i.e. heat treatment A) specimens of both CuCrZr and CuNiBe alloys (see Table 2). At the irradiation temperature of 350^{o}C, the precipitates are found to coarsen in CuNiBe as well as in CuCrZr. However, the CuNiBe alloy seems to be more sensitive to irradiation in that the precipitate density decreases, precipitate size increases and precipitation occurs at the grain boundaries as well as in the precipitate denuded zone along the grain boundaries (Fig. 1).

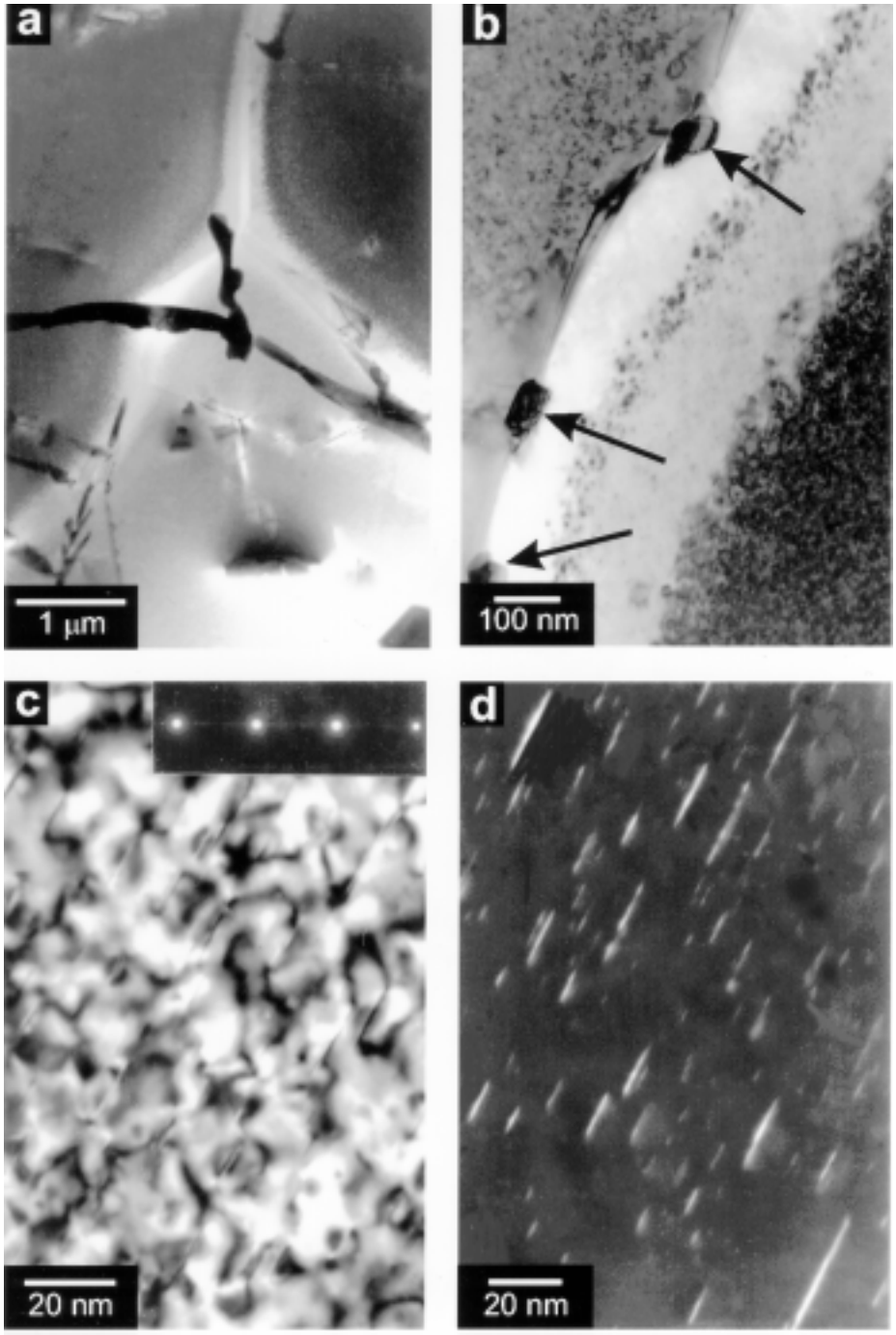

Figure 1. Microstructure of the irradiated CuNiBe (HTB) showing (a) wide denuded zones and extensive precipitation along the grain boundaries. The micrograph in (b) shows an example of a boundary that has migrated and left behind small unidentified precipitates. The γ" precipitates imaged in bright field and precipitate in dark field are shown in (c) and (d), respectively.

The post-irradiation size distribution of the precipitates in CuNiBe and CuCrZr alloys after different heat treatments are shown in Figs. 2 and 3, respectively. This evidence suggests the possibility of irradiation-induced dissolution and reprecipitation in the CuNiBe alloy.

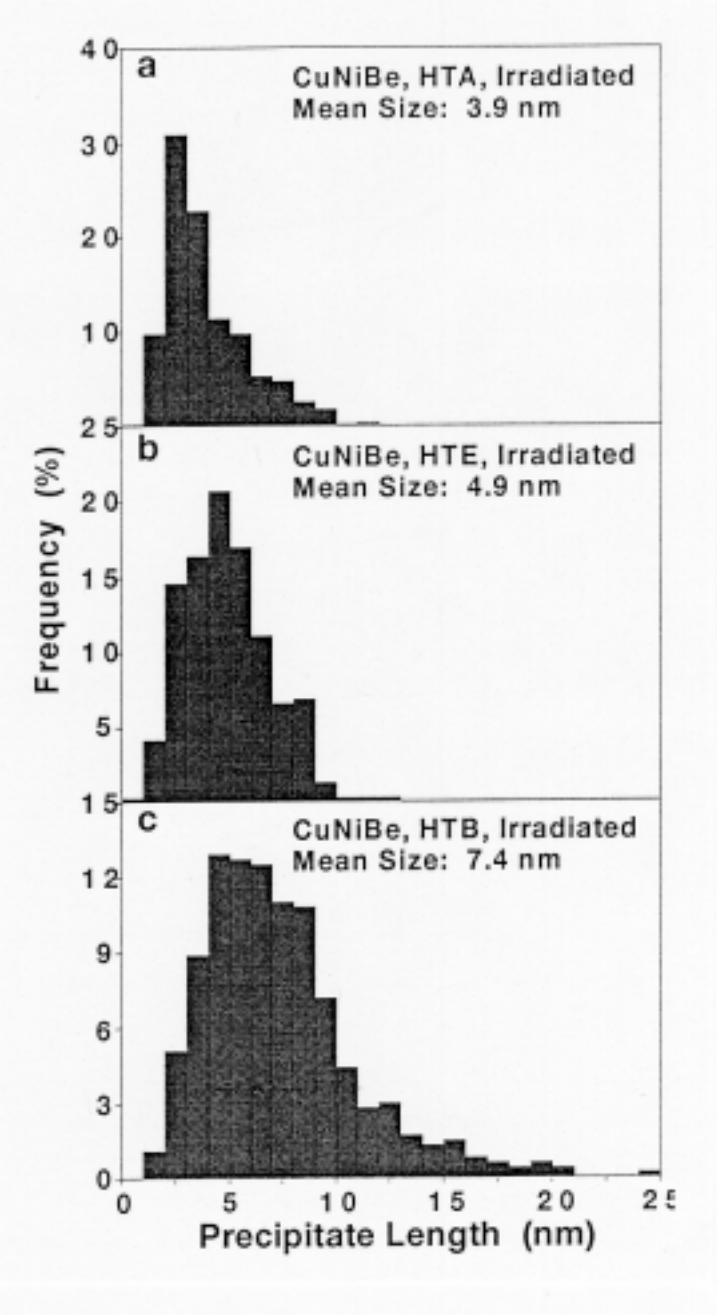

Figure 2. Size distributions for Tréfimétaux CuNiBe alloys after irradiation comparing the differences between the three different heat treatments after irradiation.

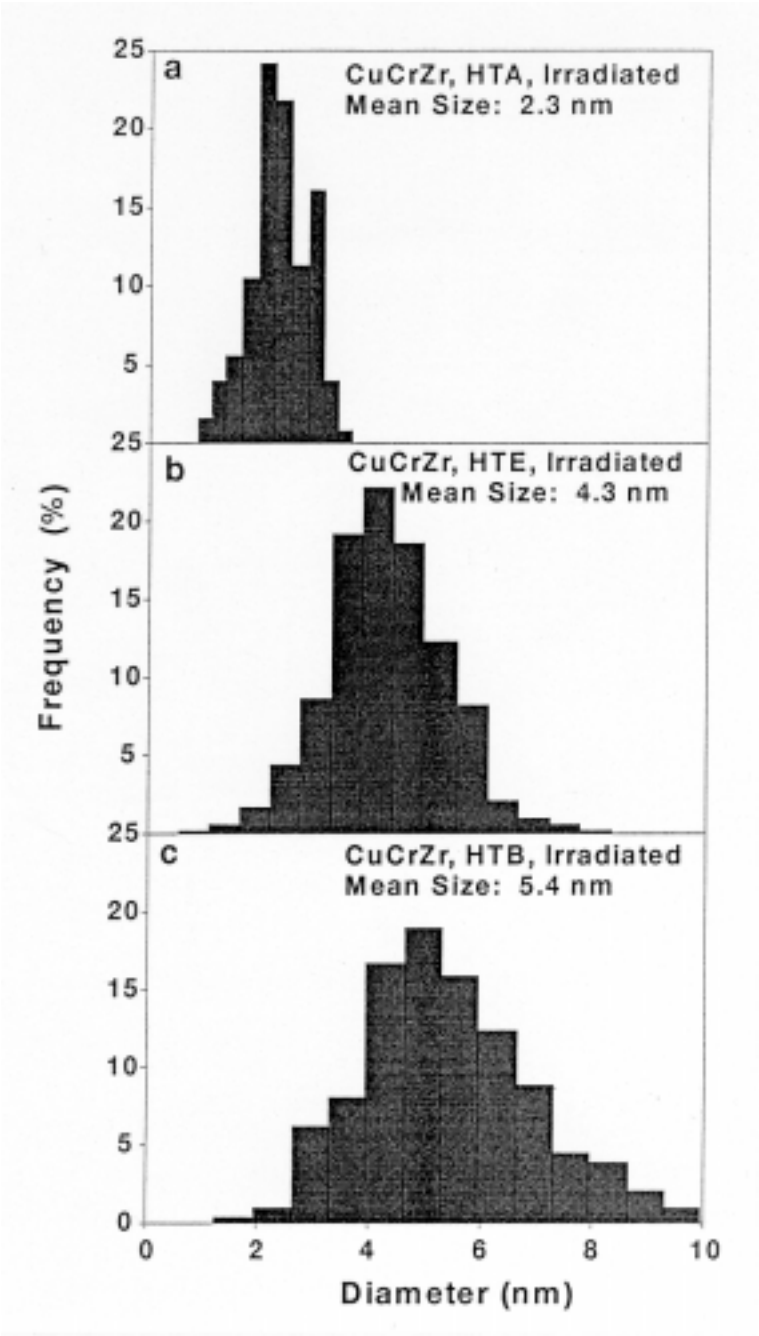

Figure 3. Size distributions for the irradiated Tréfimétaux CuCrZr alloys comparing the different heat treatments.

Heat Treatments	Tréfimétaux CuCrZr	Tréfimétaux CuNiBe	Hycon 3HP CuNiBe	Glid Cop CuAl-25
Pre-irradiation Precipitate Microstructure (10^{23} m^{-3})				
A	-	-	-	-
E	0.59 (2.9 nm)	18 (3.8 nm)	2.4 (10 nm)	-
B	0.36 (2.3 nm)	14 (6.6 nm)	-	-
C	-	13	-	-
C´	0.51	13	-	-
D	-	-	-	0.19 (6.4 nm)
Post-irradiation Precipitate Microstructure, 350°C, 0.3 dpa (10^{23} m^{-3})				
A	1.3 (2.3 nm)	6.9 (3.9 nm)	-	-
E	1.8 (4.3 nm)	6.3 (4.9 nm)	1.8 (10.8 nm)	-
B	0.29 (5.4 nm)	4.2 (7.4 nm)	-	-
D	-	-	-	0.18 (9.4 nm)

Table 2. Precipitate and particle densities and average sizes (numbers in nm in the brackets) before and after irradiation.

The results of the electrical resistivity measurements on the unirradiated as well as irradiated (at 350°C to 0.3 dpa) specimens of copper alloys are shown in Table 3. It is interesting to note that the irradiation appears to improve the electrical conductivity in CuNiBe as well as in CuCrZr; the improvement is largest in the case of CuCrZr alloys. In the case of CuNiBe (Hycon 3HP), however, the conductivity remains unchanged (Table 3).

MATERIALS	HEAT TREATMENT	IRRADIATION DOSE (dpa)	RELATIVE RESISTIVITY	RELATIVE CONDUCTI-VITY (%)
OFHC	550°C, 2h	Unirr.	1	100
CuNiBe	A	Unirr.	3.129	32.0
CuNiBe	E	Unirr.	2.345	42.6
CuNiBe	B	Unirr.	2.374	42.1
Hycon 3HP	"Prime Aged"	Unirr.	1.547	64.6
Cu-Cr-Zr	E	Unirr.	1.625	61.5
Cu-Cr-Zr	B	Unirr.	1.403	71.3
CuNiBe	A	0.3	2.062	48.5
CuNiBe	E	0.3	1.997	50.1
CuNiBe	B	0.3	1.893	52.8
Hycon 3HP	"Prime Aged"	0.3	1.523	65.7
Cu-Cr-Zr	E	0.3	1.294	77.3
Cu-Cr-Zr	B	0.3	1.183	84.5

Table 3. Electrical Resistivity and Conductivity for Copper Alloys Irradiated at 350°C to a Dose Level of 0.3 dpa.

The deformation behaviour of unirradiated and irradiated OFHC-copper and different copper alloys during tensile testing at 350°C is illustrated in Figs. 4 - 6. Fig. 4 shows that even OFHC-copper suffers a substantial loss in the uniform elongation due to irradiation at 350°C. In the case of CuCrZr (Fig. 5) the bonding thermal cycle (HTB) reduces the strength noticeably at 350°C. The bake-out heat treatments (C and C´), on the other hand, increases the strength almost to the level of the prime-aged strength (HTE). As can be seen in Fig. 5 (c), the CuCrZr alloy retains its ductility and ability to work harden after irradiation at 350°C.

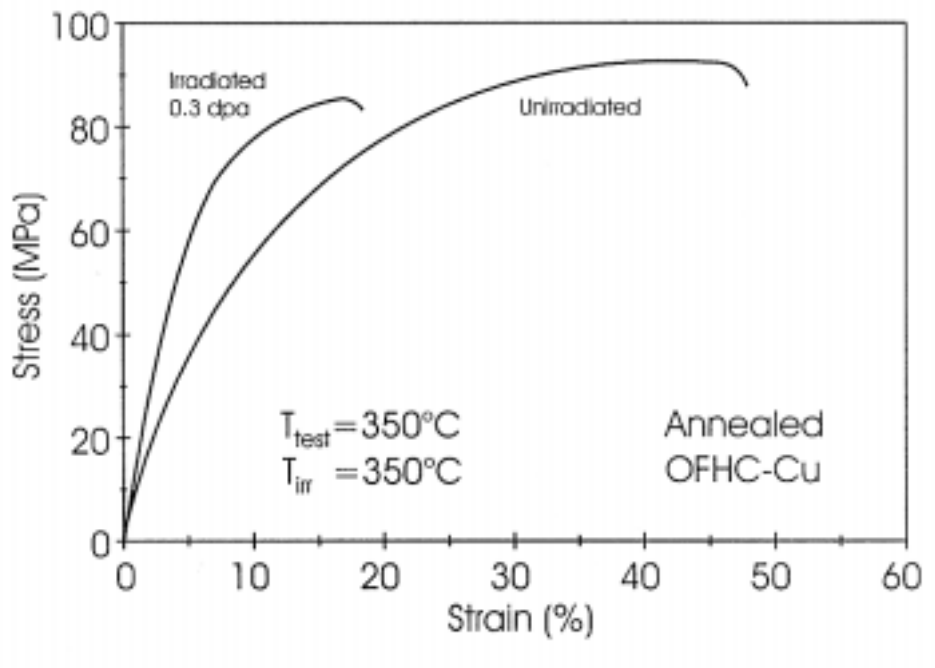

Figure 4. Stress-strain curves for the unirradiated and irradiated OFHC-Cu. Note, that the irradiation with neutrons, even at a relatively high temperature, causes a significant decrease in the ductility.

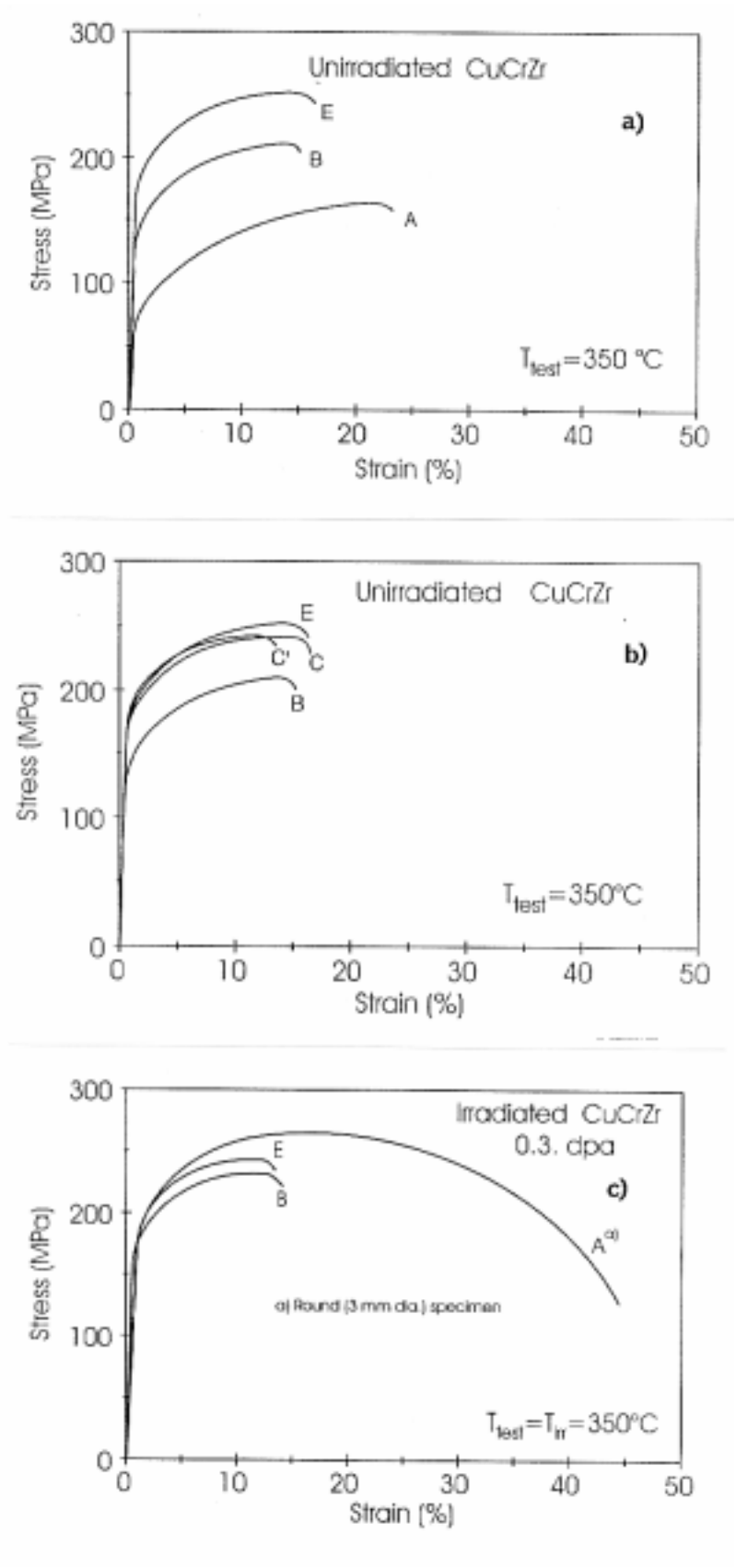

Figure 5. Stress-strain curves for the unirradiated (a, b) and irradiated (c) CuCrZr tested at 350°C.

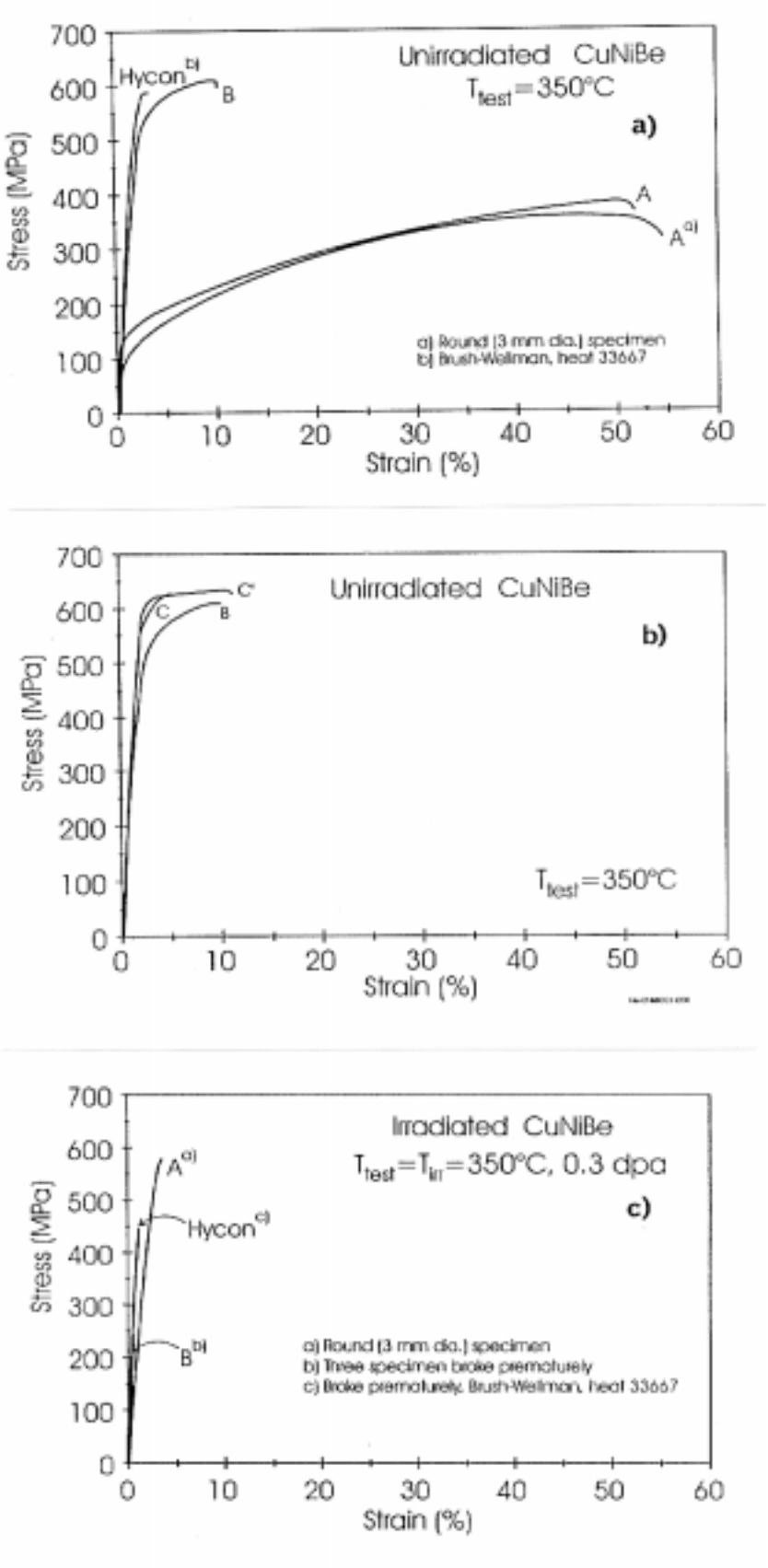

Figure 6. Stress-strain curves for the unirradiated (a, b) and irradiated (c) CuNiBe tested at 350°C.

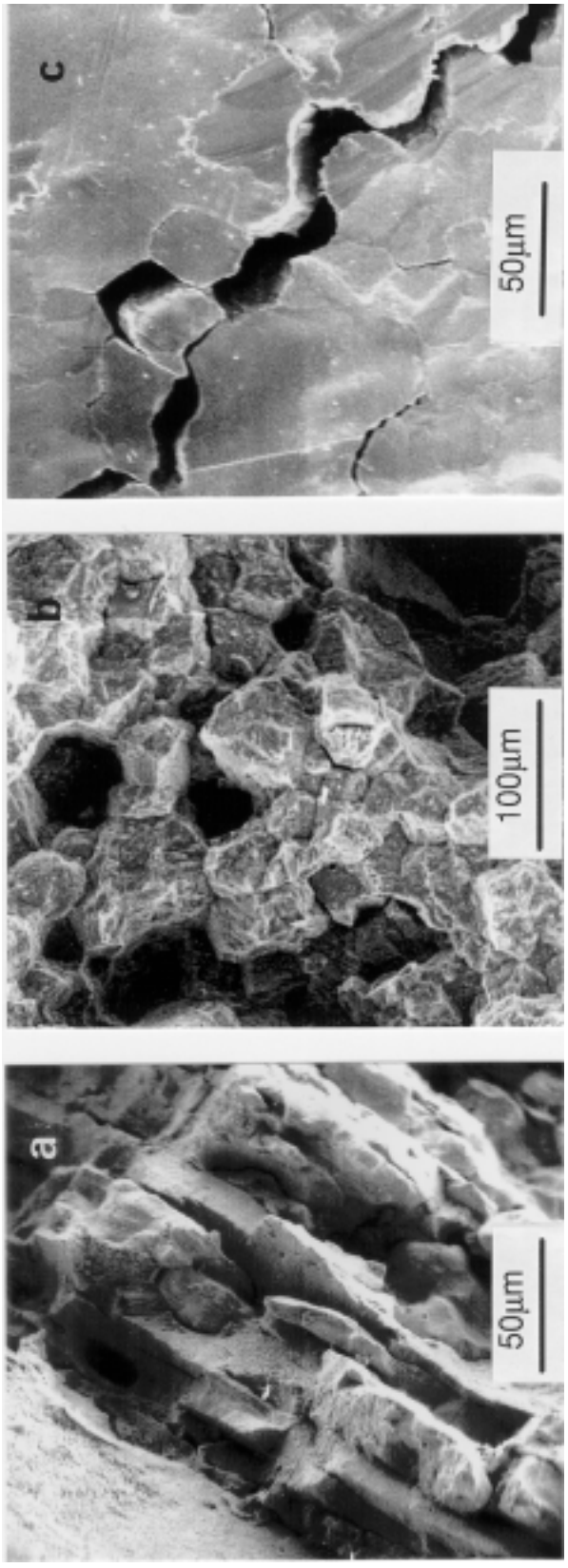

Figure 7. Fracture surfaces from the irradiated CuNiBe specimens with solution annealing (HTA) (Fig. 7a) and bonding thermal cycle (MTB) treatments (Fig. 7b); Fig. 7c shows the surface of the specimen shown in Fig. 7b. Note the intergranular mode of failure.

The situation in the case of CuNiBe alloys is significantly different (see Fig. 6). Even in the unirradiated state these alloys after various heat treatments (other than solution annealing, HTA) seem to have a very limited capability to deform plastically (Fig. 6 a, b). Irradiation at 350°C renders these alloys completely brittle. Fractographs shown in Fig. 7 clearly demonstrate that these alloys fracture in a brittle manner where grains are pulled apart without any plastic deformation.

The CuAl-25 proved to be resistant to any significant changes in the overall strength and ductility due to the annealing treatment (HTD) and irradiation at 350°C to a dose level of 0.3 dpa. The results shown in Fig. 8 provide evidence for irradiation-induced softening in the highly cold-worked (HTD´) CuAl-25. The strength of the annealed CuAl-25 (HTD) does not seem to be affected by the irradiation at 350°C. The uniform elongation is not affected by the irradiation either and in both cases (i.e. HTD and HTD´) the fracture occurs in a ductile manner.

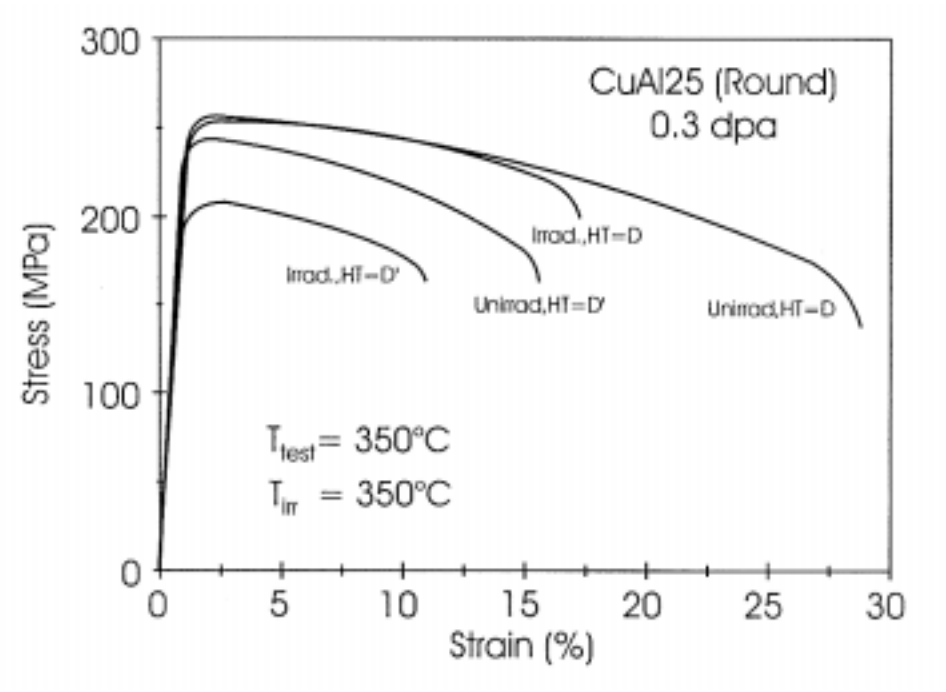

Figure 8. Stress-strain curves for the unirradiated and irradiated CuAl-25 tested at 350°C.

3.2.2 Low Cycle Fatigue Behaviour of Unirradiated and Irradiated Copper and Copper Alloys.

B.N. Singh, J.F. Stubbins, and P. Toft (*University of Illinois, USA)*

Specimens of OFHC-copper, dispersion strengthened CuAl-25 and precipitation hardened CuCrZr were irradiated at ~47 and 100°C in the DR-3 reactor at Risø to a displacement dose level of ~0.3 dpa. The results on the fatigue lifetime of these materials as a function of stress amplitude were reported last year. These results indicated that the irradiation did not cause any degradation in the lifetime of these materials; if anything, the

lifetime of the irradiated CuAl-25 seemed to have improved. To understand this behaviour, further experiments were carried out on unirradiated and irradiated specimens of OFHC-copper, CuAl-25 and CuCrZr. From these cyclic step experiments, the cyclic hardening behaviour was established and compared directly with the monotonic hardening behaviour from the results of tensile tests on the same materials with the same irradiation conditions.

The stress-strain curves determined from the cyclic step experiments carried out at room temperature on different materials in the unirradiated and irradiated conditions are shown in Fig. 9. Fig. 10 shows the plastic components of the stress-strain curves for the cyclic step tests as well as monotonic (tensile) tests at room temperature on OFHC-copper and CuAl-25 specimens in the unirradiated and irradiated conditions. These results indicate that while the unirradiated materials tend to cyclically harden, the cyclic step tests following irradiation at ~47^{o}C induce a gradual softening. These results can be understood in the light of the fatigue-induced microstructural evolution in these materials. In all cases, fatigue loading tends to induce flow which clears the irradiation-induced defect clusters. Evidently, dislocation sweeping is effective in reducing obstacles to plastic flow and reduces the tendency for the flow localization, which is found in the monotonic loading conditions. The reduction in the density of obstacles to plastic flow during cyclic step tests may be the reason for the lower stress level reached in the cyclic step experiments than in the corresponding monotonic tensile experiments (Fig. 10).

Further analysis of the results of the cyclic step experiments shows that the results of fatigue experiments carried out in the stress-controlled mode can be directly compared with the results of fatigue experiments carried out in the strain-controlled mode. Furthermore, these analyses show that the fatigue lines of the copper alloys, CuCrZr and CuAl-25, are controlled primarily by the elastic response, which is directly proportional to stress.

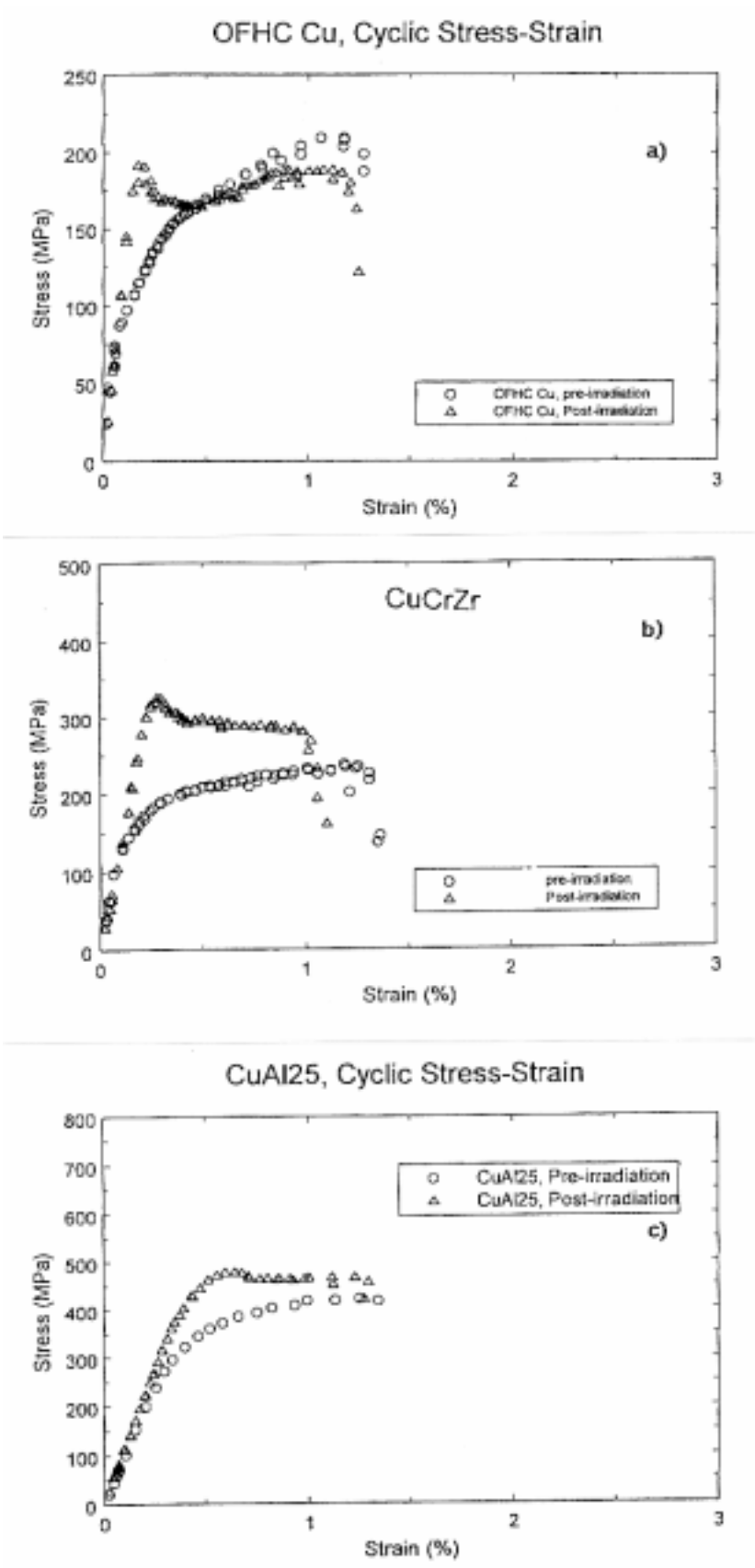

Figure 9. Cyclic stress-strain curves for (a) 8FHC-Cu, (b) CuCrZr, and (c) CuAl-25 determined at room temperature in the unirradiated and irradiated conditions. Specimens were irradiated at ~47^{o}C to 0.3 dpa.

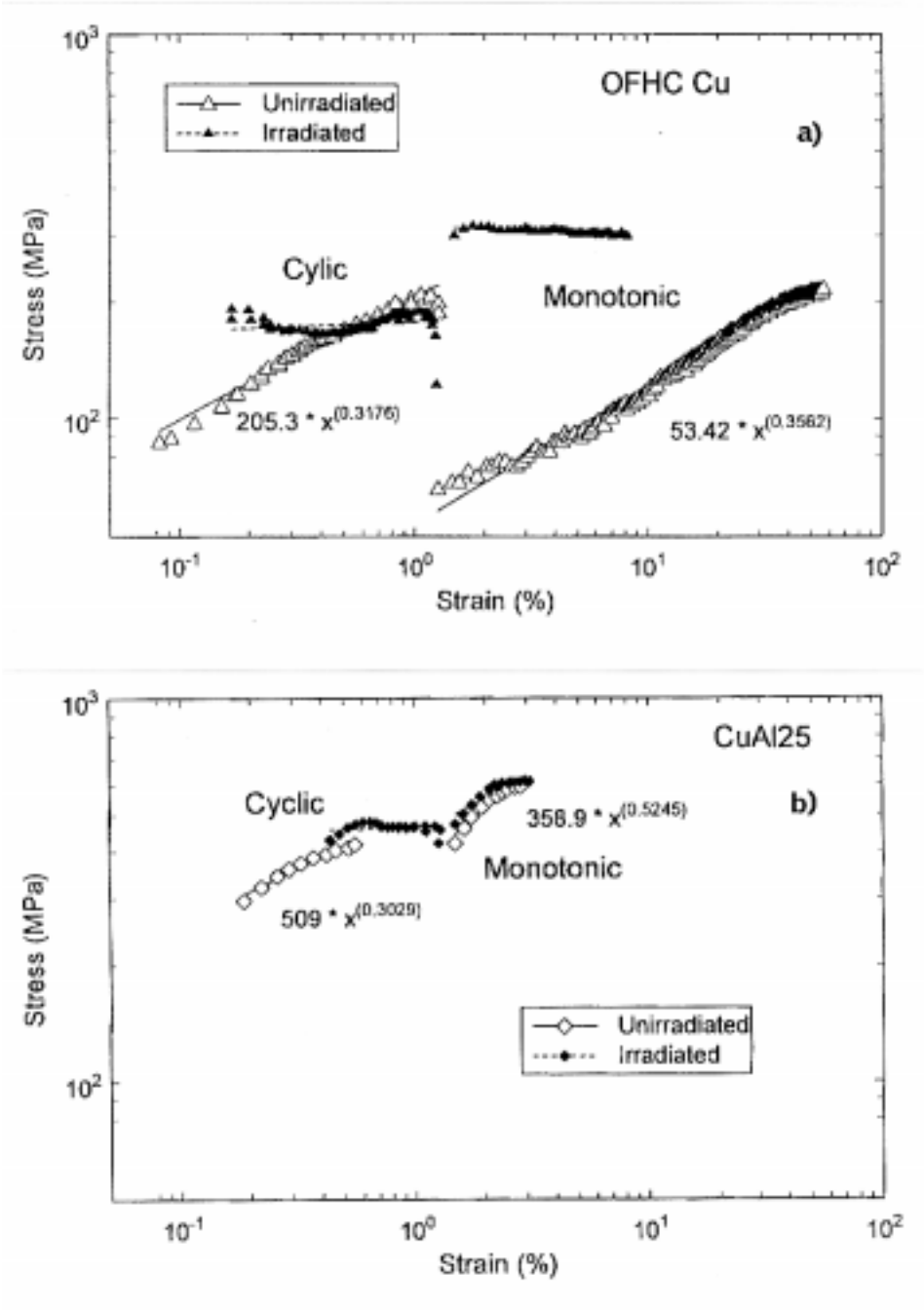

Figure 10. Plastic components of the stress-strain curves for (a) OFHC-Cu and (b) CuAl-25 for cyclic and monotonic testing modes.

3.2.3 Influence of Nickel on Swelling Behaviour of Copper Irradiated with Neutrons

B.N. Singh, F.A. Garner, D.J. Edwards* and J.H. Evans** (*Pacific Northwest National Laboratory, USA; **University of London, England).*

When pure copper is irradiated with neutrons, the elements nickel, zinc and cobalt are formed by transmutation. It is expected that during the lifetime of ITER, a considerable amount of nickel will be produced in the copper and copper alloys used in different components of ITER. It was, therefore, decided to study the influence of nickel on the swelling behaviour of copper.

Five Cu - x Ni alloys, where x = 0.17, 1.0, 2.0, 5.0, and 10 weight percent, were irradiated in COBRA-1A in the EBR-II reactor at about 390 and 500^{o}C to a fluence level of 17.8 x 10^{25} n/m^{2} (E > 0.1 MeV) corresponding to a displacement damage level of 11.3 dpa (NRT). Transmission electron microscopy (TEM) was used to determine the effect of irradiation on the dislocation microstructure and void swelling of these alloys. The main results are quoted in Table 4. The results show that the void size and swelling at 390^{o}C increase between 0 and 1% Ni and then decreases rapidly with increasing Ni content. The void density, on the other hand, first decreases and then increases with the Ni content. At the irradiation temperature of 500^{o}C (also 11 dpa) only a few voids were observed. Some bubbles were seen at grain boundaries. A few relatively small bubbles were observed in the grain interiors, particularly at dislocation and dislocation junctions.

The general trend of variation of void size, density and swelling with Ni content during neutron neutron irradiation is found to be very similar to that observed in the case of 1 MeV electron irradiation of these alloys. The results indicate a temperature shift of ~100^{o}C for all void parameters between the 1 MeV electron and fission neutron irradiation. The swelling rate (per dpa) is significantly higher in the neutron than in the electron irradiated copper and Cu-Ni alloys. This is true even when the effects of damage rate on the mutual recombination and temperature shift are taken into account. This difference becomes even more significant when it is considered that the damage production efficiency in the case of electron irradiation is about 10 times higher than that during neutron irradiation.

PARAMETERS	MATERIALS				
	OFHC Copper	**Cu-1% Ni**	**Cu-2% Ni**	**Cu-5% Ni**	**Cu-10% Ni**
Void Size (nm)	315	549	262	190	176
Void Density (m^{-3})	$4.3x10^{18}$	$1.3x10^{18}$	$7.6x10^{18}$	$1.0x10^{19}$	$6.1x10^{18}$
Void Swelling (1%)	7.6	12.8	7.8	3.9	1.8
Swelling Rate (%/dpa)	0.69	1.16	0.71	0.35	0.16
Swelling Rate (1 MeV $\bar{e}$ at 500°C) (% dpa)	0.09	0.2	0.31	0.16	~0

Table 4. Void size, density and swelling measured by TEM on pure copper and CuNi alloys irradiated at 393°C to a displacement dose level of 11.3 dpa.

3.3 Long-Term Technology

3.3.1 Effect of Irradiation on Mechanical Properties of Iron and Low Activation steels

B.N. Singh, A. Horsewell and P. Toft

Tensile specimens of pure iron (0.25 mm thick), modified F82H (0.3 mm thick) and MANET-2 (0.3 mm thick) were fabricated from the as-supplied materials. The tensile specimens of pure iron were annealed at 650°C for 2 h (in vacuum of ~10^{-6} torr) before irradiation and tensile testing in the unirradiated conditions. Tensile specimens of the modified F82H and MANET-2 were irradiated and tensile tested (in the unirradiated condition) in the as-supplied condition.

Tensile specimens of pure iron were irradiated with fission neutrons in the DR-3 reactor at Risø ((a) at 50°C to dose levels of ~0.01, 0.1 and 0.5 dpa, and (b) at 250°C to dose levels of 0.1 and 0.3 dpa. Tensile specimens of modified F82H and MANET-2 steels were irradiated at 250°C to dose levels of 0.1 and 0.3 dpa. All irradiation experiments were carried out with a damage rate of ~5 x 10^{-8} dpa/s.

Both unirradiated and irradiated specimens of pure iron, modified F82H and MANET-2 were tested in an Instron machine at a strain rate of

1.3 x 10^{-3} s^{-1}. In all cases, irradiated and unirradiated specimens were tested at the irradiation temperature. In addition, tensile specimens of unirradiated modified F82H and MANET-2 were tested at 22, 250 and 350°C. All tests were carried out in vacuum (10^{-5} torr).

At the irradiation and test temperature of ~50°C (Fig. 11), the effects of irradiation on the deformation behaviour of pure iron became clearly visible already at the dose level of 0.01 dpa. The most striking feature of these results is the absence of work hardening in the irradiated specimens. It should be noted, however, that at the dose level of 0.5 dpa, there is an indication of some work hardening. It is also of interest to note that the magnitude of yield drop increases with increasing dose level (Fig. 11).

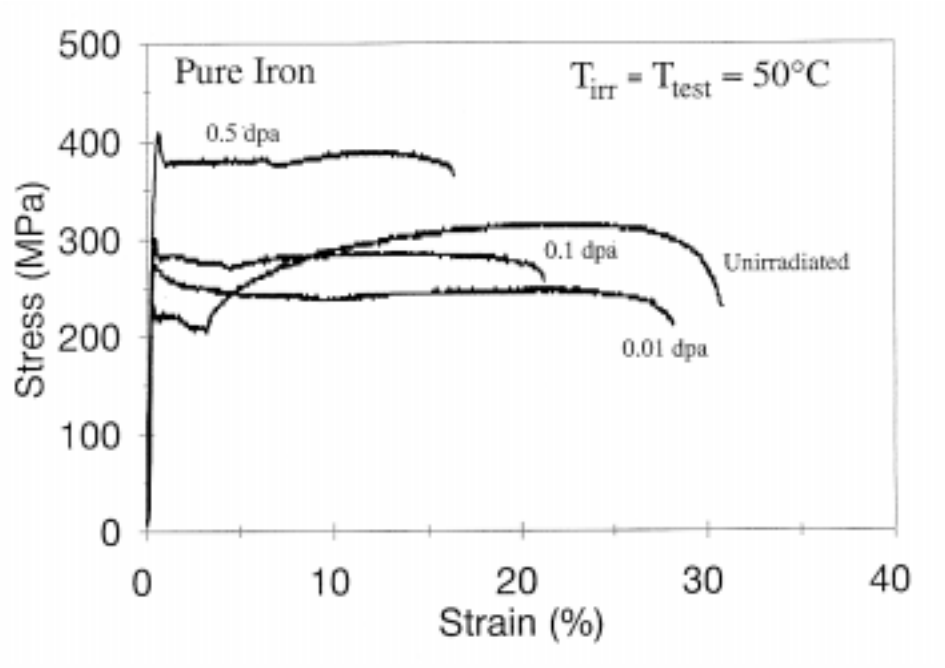

Figure 11. Stress-strain curves for pure iron irradited with fission neutrons at ~47°C to doses of 0.01, 0.1 and 0.5 dpa.

The specimens of pure iron irradiated and tested at 250°C show a somewhat unusual behaviour in that the ultimate tensile strength (σ_{max}) of the irradiated specimens are found to be lower than that of the unirradiated ones. This is the result of a reduction in work hardening rate due to irradiation. The observed increase in the yield stress due to irradiation is consistent with the commonly expected effect of irradiation on hardening. It may be significant that at the dose level of 0.3 dpa, there is a clear indication of an upper yield point and a small but finite Lüders strain.

The effect of irradiation on deformation behaviour of MANET-2 irradiated and tested at 250°C to dose levels of 0.1 and 0.3 dpa is shown in Fig. 12. It can be seen, that both $\sigma_{0.2}$ and σ_{max} increase with irradiation dose level. It is important to note that the uniform elongation is not affected by irradiation.

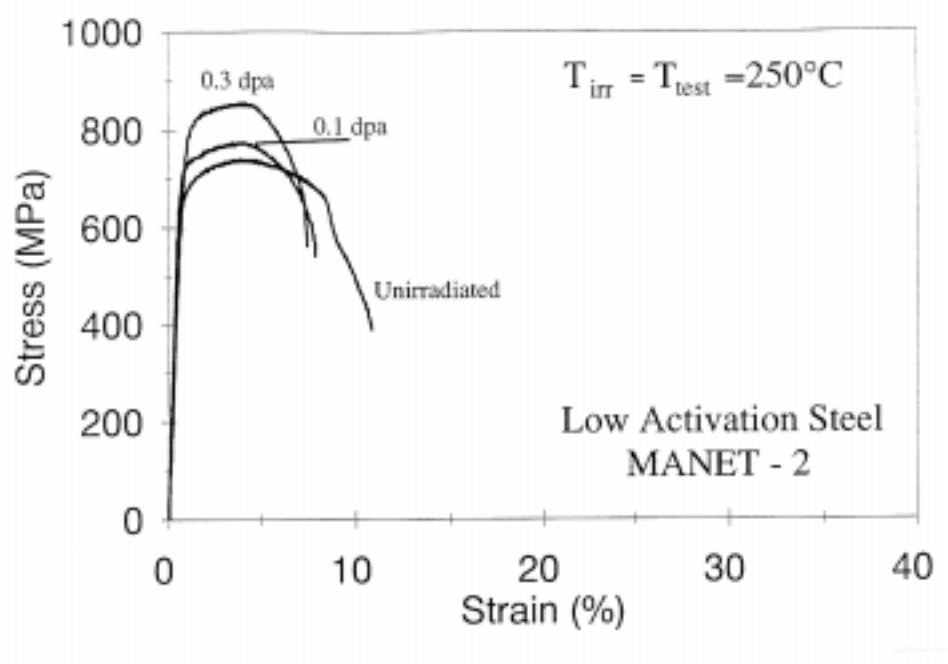

Figure 12. Stress-strain curves for the unirradiated and irradiated low activation steel, MANET-2. Irradiation and tensile testing were carried out at 250°C.

The specimens of modified F82H irradiated and tested at 250°C showed no clear effect of irradiation on hardening or elongation.

3.3.2 Cascade-Induced Source Hardening Model

B.N. Singh, A.J.E. Foreman and H. Trinkaus** (*Forschungszentrum Jülich, Germany, **AEA Technology, Harwell, England)*

The problem of radiation hardening has been a subject of both experimental and theoretical investigations for a long time. A close and critical analysis of the available literature on this topic shows, however, that the deformation behaviour of irradiated metals and alloys is still not clearly understood. The analysis identified a number of important features of the post-irradiation deformation behaviour that cannot be rationalised in terms of the traditional "dispersed barrier hardening" (DBH) model. The DBH model assumes that the irradiation-induced clusters/loops would act as Orowan type of obstacles and that the pre-irradiation microstructure contains a high density of grown-in dislocations. The present work has demonstrated that neither of these assumptions are valid.

In the present study, we consider an alternative proposition that the irradiation-induced increase in the yield stress (i.e. the stress necessary to initiate the plastic flow) may occur simply because most of the Frank-Read (F-R) sources (i.e. grown-in dislocations) are "locked" during irradiation. The locking is considered to occur during very early stages of irradiation by the accumulation of small clusters/loops of self-interstitial atoms (SIA) in the vicinity of grown-in dislocations. The SIA clusters are assumed to arrive via one-dimensional glide and accumulate at a certain distance - stand-off distance - from the grown-in dislocation. Calculations

show that the small loops at a distance smaller than the stand-off distance get sucked into the dislocation core due to the large elastic force field of the grown-in dislocation. Two possibilities for the physical absorption of small loops into the dislocation core are considered. First, the elastic force field is strong enough to realign the Burgers vector of the small loops such that they glide into the core of the lead dislocation. An alternative mechanism of the loop absorption at a grown-in dislocation may be the break-up of small SIA loops under the combined influence of a large hydrostatic tension from the dislocation and the ambient temperature (Fig. 13). Once an SIA breaks loose from the loop, it can readily escape from the loop and get absorbed into the core of the grown-in dislocation.

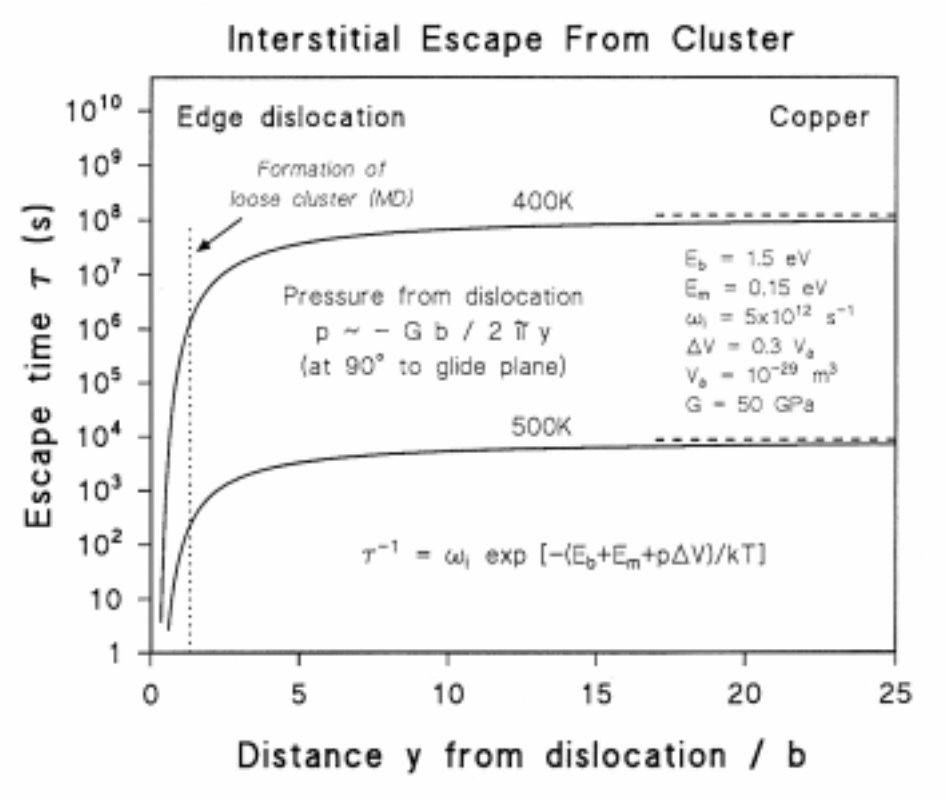

Figure 13. The dependence of the escape time for an interstitial atom from a small SIA loop on the distance from an edge dislocation in copper under the influence of the ambient temperature and hydrostatic tension.

In the present model, the initiation of the plastic flow and the upper yield stress is related to the breakaway stress which is necessary to pull the grown-in dislocation away from the atmosphere of loops decorating it. The magnitude of the breakaway stress has been calculated in terms of the stand-off distance, the size of loops and the distance between the loops decorating the dislocation. The calculated stress values are found to be in good agreement with the measured increase in the initial yield stress in neutron irradiated copper.

3.4 Underlying Technology

3.4.1 Effect of post-irradiation annealing

B.N. Singh, M. Eldrup and P. Toft

It is well known that copper and copper alloys suffer a severe loss of ductility due to irradiation at temperatures below about 200°C. The loss of ductility is caused by the accumulation of the irradiation-induced defects. In pure copper these defects can be removed by post-irradiation annealing at temperatures above 250°C and thereby the ductility can be recovered. Whether or not this can be achieved in the case of CuCrZr, CuNiBe and CuAl-25 alloys is not known. It would be of a great advantage, if this could be achieved since the components containing these materials in ITER could be periodically annealed to regain the ductility.

To test out this possibility, specimens of different copper alloys were irradiated at 100°C to displacement doses of 0.2 and 0.3 dpa. Tensile properties and electrical resistivity of these specimens were determined in the unirradiated and irradiated conditions. Some of the irradiated specimens were then annealed at 300°C for 50 h in vacuum. The tensile properties and electrical resistivity of these specimens were determined in the irradiated and annealed condition. Some reference unirradiated specimens were also annealed at 300°C for 50 h and their properties were determined before and after annealing. The experiments on CuCrZr and CuAl-25 alloys have been completed. The electrical conductivity results are shown in Table 5. These results clearly show that in all cases the post-irradiation annealing at 300°C for 50 h leads to an increase in the conductivity indicating the recovery of the irradiation-induced defects.

The effect of annealing and post-irradiation annealing on the deformation behaviour of the prime-aged (HTE) CuCrZr is illustrated in Fig. 14. It can be seen that the annealing of the unirradiated specimens leads to a small decrease in the ultimate strength of the material but the ductility remains unaffected (Fig. 14a). The post-irradiation, on the other hand, has most stronger effect on the strength as well as the uniform elongation. In fact, the ductility of the irradiated CuCrZr recovers to the extent where it can be used without any serious concern regarding its mechanical performance. It should be noted, however, that the recovery in the strength due to the post-irradiation annealing is noticeably less in the specimens irradiated to 0.3 dpa than in the specimens irradiated to 0.2 dpa.

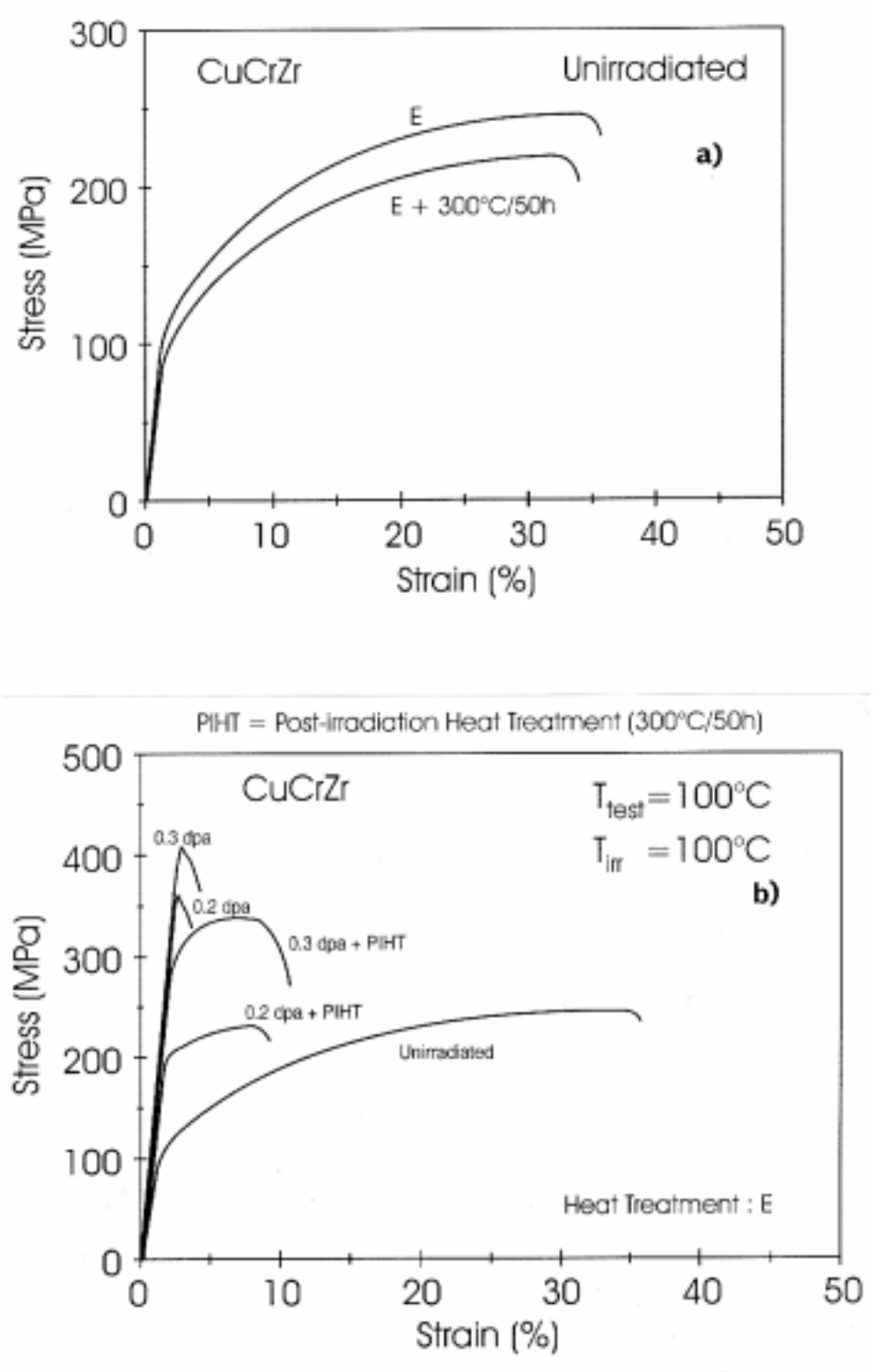

Figure 14. Deformation behaviour of CuCrZr in the as-irradiated and after post-irradiation annealing (at 300°C for 50 h) conditions. The results on unirradiated and heat-treated CuCrZr are also shown.

Material	Heat Treatment	Irradiation Dose (dpa)	Irr. Temp. (^{0}C)	Relative conductivity (%)			
				As prep.	As prep. +annealed	As irradiated	Irradiated +annealed
CuCrZr	A	0.3	100	47.9	-	55.1	67.8
"	B	0.3	"	59.5	-	72.0	76.3
"	C	0.3	"	78.8	-	65.2	72.8
"	E	0.2	"	-	-	53.8	66.0
"	E	0.3	"	52.2	55.9	60.8	69.1
CuAl-25	D	0.2	"	-	-	80.4	82.2

Table 5. Relative conductivity results for "as-prepared", "annealed" (300^{o}C, 50 h), "as irradiated" and irradiated and subsequently annealed at 300^{o}C for 50 h.

3.4.2 Damage Accumulation in single crystal, polycrystal and cold-worked copper irradiated with fission neutrons

B.N. Singh, M. Eldrup and S.J. Zinkle (*Oak Ridge National Lab., USA)*

The consideration of intracascade clustering of self-interstitial atoms (SIAs) and vacancies and thermal stability of these clusters has led to the concept of "production bias". Within this framework, one-dimensional glide of SIA loops plays a crucial role in the evolution of the defect microstructure. This immediately implies that a quantitative description of the damage accumulation under cascade damage conditions must include considerations of one-dimensional motion of small SIA loops. Under these conditions, the nature and concentration of pre-irradiation sinks may determine the efficiency of defect accumulation in the form of clusters, loops, dislocation segments and voids. The present experiments were designed to investigate the influence of well defined sinks such as grain boundaries and dislocations on the accumulation of SIAs and vacancies during neutron irradiation.

Samples of high purity copper in single crystal, polycrystal and cold-rolled (~85%) conditions were irradiated with fission neutrons at 350^o in the DR-3 reactor at Risø. To ensure identical irradiation conditions, all samples were loaded in one single capsule in the high temperature rig where the irradiation temperature is measured and controlled continuously. Specimens were irradiated to a displacement dose level of ~0.3 dpa (NRT). Irradiated specimens were examined in the JEOL 2000 FX transmission electron microscope (TEM). Defect microstructure (cluster/loop density, cluster size, dislocation density, void size and density) were quantitatively characterised. In addition, positron annihilation spectroscopy technique was used to characterise the defect microstructures in the bulk.

The post-irradiation TEM investigations showed that the cold-worked copper recrystallized even before the reactor was brought to full power

(10 MW). This meant that the cold-worked material was irradiated in the recrystallized state. The resulting grain size was found to be in the range 0.5 - 5 μm. After irradiation the dislocation density (ρ) in the single crystal, polycrystal and cold-worked and recrystallized specimens was practically the same (see Table 6). This means that the main variable in these experiments was the grain size. Both void density and swelling increase with decreasing grain size (see Table 6). These TEM observations are confirmed by the positron annihilation experiments on the bulk specimens.

The results could be easily understood in terms of production bias model and are consistent with the hypothesis that the one-dimensional glide of small SIA clusters plays a crucial role in defect accumulation.

PARAMETERS	MATERIALS		
	Single Crystals	Polycrystals (OFHC)	Polycrystals (OFHC) Cold-worked
$\bar{d}_v$ (nm)	86.9	90.0	92.2
$3\sqrt{d_v^3}$ (nm)	95.3	105.5	104.5
$C_v(10^{18}\ m^{-3})$	2.0	4.9	7.4
S_v (%)	0.10	0.30	0.44
ρ $(10^{12}\ m^{-2})$	2	~4[(a)]	~4[(a)]
C_{cl} $(10^{21}\ m^{-3})$	1[b)]	2[(b)]	2[(b)]
$\bar{d}_{cl}$ (nm)	3.4	3.4	3.4

(a) including handling dislocations, the real density may be close to 2 x 10^{12} m^{-2}, as for the single crystal specimens. (b) ≥80% of clusters are SFT; the fraction may be as high as 95%.

Table 6. TEM results on void size ($\bar{\mathbf{d}}_v$), density (C_v), swelling (S_v), dislocation density (ρ), cluster density (C_{cl}) and cluster size ($\mathbf{d}_{cl}$) for copper irradiated at 350°C to a dose level of 0.3 dpa.

3.4.3 **Stochastic Annealing Simulation of Intracascade Defect Interactions**

H.L. Heinisch and B.N. Singh (*Pacific Northwest National Laboratory, USA)*

Atomic scale computer simulations are used to investigate the intracascade evolution of the defect populations produced in cascades in copper over macroscopic time scales. Starting with cascades generated using molecular dynamics (MD), the diffusive transport and interactions of the defects are followed for hundreds of seconds in stochastic annealing simulations. The temperature dependencies of annihilation, clustering and free defect production are determined for individual cascades, especially including the effects of the subcascade structure of

high energy cascades. The subcascade structure is simulated by closely spaced groups of lower energy MD cascades.

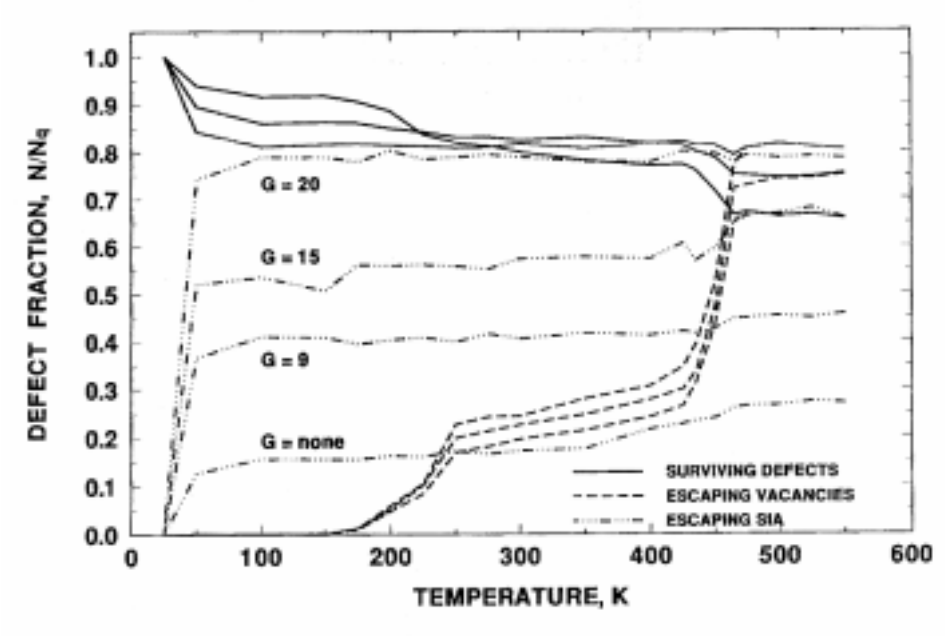

Figure 15. The fractions of point defects surviving recombination and of vacancies and interstitials escaping from 25 keV cascades in copper during the annealing stage, as a function of cascade annealing temperature. G is the number of interstitial atoms in the gliding SIA clusters.

The simulation results illustrate the strong influence of the defect configuration existing in the primary damage state on subsequent intracascade evolution. The results summarised in Fig. 15 show that all SIA clusters that are taken to be glissile quickly escape the cascade region at virtually any temperature above 50 K. The fraction of escaping SIAs in these 25 keV copper copper cascades varies from 10% - 80%, depending on the maximum size assumed for glissile clusters. Thus, the fraction of escaping SIAs during annealing stage depends on both the mobility of SIA clusters as a function of size and the size distribution of SIA clusters in cascades after quenching. It is concluded that the existence of glissile SIA clusters, formed directly in cascades, and the characteristics of their motion are extremely important elements in determining the mobile defect fractions from individual cascades and the nature of the global defect population.

3.5 Participants in Fusion Technology

Scientific Staff
Eldrup, Morten (part time, ~70%)
Horsewell, Andy (part time, ~20%)
Singh, Bachn N.
Toft, Palle (part time, ~50%)

Technical Staff
Lindbo, Jørgen (part time, ~20%)
Nilsson, Helmer (part time, ~10%)
Olsen, Benny F.
Pedersen, N.J. (part time, ~40%)

Guest Scientists
Edwards, D.J., Pacific Northwest National Laboratory, Richland, USA
Evans, John H., University of London, England
Golubov, S.I., Institute of Physics and Power Engineering, Obninsk, Russia
Heinisch, H.L., Pacific Northwest National Laboratory, Richland, USA
Stubbins, J.F., University of Illinois, Urbana-Champaign, USA
Zinkle, S.J., Oak Ridge National Laboratory, Oak Ridge, USA

3.6 Publications and Conference Contributions

3.6.1 Publications

Fabritsiev, S.A.; Pokrovsky, A.S.; Zinkle, S.J.; Rowcliffe, A.F.; Edwards, D.J.; Garner, F.A.; Sandakov, V.A.; Singh, B.N.; Barabash, V.R., Tensile and electric properties of copper alloys irradiated in a fission reactor. In: Fusion materials. Semiannual progress report for the period ending December 31, 1995. DOE-ER-0313/19 (1996) p. 177-188

Fabritsiev, S.A.; Zinkle, S.J.; Singh, B.N., Evaluation of copper alloys for fusion reactor divertor and first wall components. J.Nucl. Mater. (1996) v. 233/237 p. 127-137.

Fabritsiev, S.A.; Pokrovsky, A.S.; Zinkle, S.J.; Rowcliffe, A.F.; Edwards, D.J.; Garner, F.A.; Sandakov, V.A.; Singh, B.N.; Barabash, V.R., The effect of neutron spectrum on mechanical and physical properties of pure copper and copper alloys. J. Nucl. Mater. 233-237 (1996) 526-533.

Heinisch, H.L.; Singh, B.N., Stochastic annealing simulation of differential defect production in high energy cascades. J. Nucl. Mater. (1996) v. 232 p. 206-213.

Kirkegaard, P.; Eldrup, M.; Horsewell, A.; Pedersen, J.S., Correlation of bubble size distributions from transmission electron microscopy observations. Risø-R-789 (EN) (1996) 43 p.

Leedy, K.D.; Stubbins, J.F.; Singh, B.N.; Garner, F.A., Fatigue behaviour of copper and selected copper alloys for high heat flux applications. J. Nucl. Mater. (1996) v. 233/237 p. 547-552

Lynov, J.P.; Singh, B.N. (eds.), Association Euratom - Risø National Laboratory annual progress report 1995. Risø-R-897(EN) (1996) 70 p.

Singh, B.N.; Edwards, D.J.; Horsewell, A.; Toft, P., Dose dependence of microstructural evolution and mechanical properties of neutron irradiated copper and copper alloys. (ITER R&D Task no. T13). Risø-R-839(EN) (1995) 34 p.

Singh, B.N.; Edwards, D.J.; Toft, P., Effects of neutron irradiation on mechanical properties and microstructures of dispersion and precipitation hardened copper alloys. J. Nucl. Mater. (1996) v. 238 p. 244-259

Singh, B.N.; Eldrup, M., Fusionsenergi udfordrer materialeforskerne. Risø Nyt (1996) (no.4) p. 12-13

Thorsen, P.A.; Bilde-Sørensen, J.B.; Singh, B.N., Influence of grain boundary structure on bubble formation behaviour in helium implanted copper. Mater. Sci. Forum (1996) v. 207/209 p. 445-448

Trinkaus, H.; Singh, B.N.; Victoria, M., Microstructural evolution adjacent to grain boundaries under cascade damage conditions and helium production. J. Nucl. Mater. (1996) v. 233/237 p. 1089-1095

Woo, C.H.; Singh, B.N.; Semenov, A.A., Recent advances in the understanding of damage production and its consequences on void swelling, irradiation creep and growth. J. Nucl. Mater. (1996) v. 239 p. 7-23

3.6.2 Conference Contributions

Borring, J., PM used in the production of nuclear fuel element. Joint Nordic conference in powder technology, Copenhagen (DK), 13-14 Nov 1996. Unpublished.

Eldrup, M.; Singh, B.N., Studies of defects and defect agglomerates by positron annihilation spectroscopy. International workshop on defect production, accumulation and materials performance in irradiation environment, Davos (CH), 2-8 Oct 1996. Unpublished. Abstract available

Golubov, S.I.; Singh, B.N.; Trinkaus, H.; Barashev, A.V., Accumulation of radiation induced defects due to production bias and glide of small interstitial clusters. In: Program and abstracts for the 18th symposium on effects of radiation on materials. 18. Symposium on effects of radiation on materials, Hyannis, MA (US), 25-27 Jun 1996. (ASTM, Philadelphia, PA, 1996) p. 41

Heinisch, H.L.; Singh, B.N., Defect interactions within a group of subcascades using stochastic annealing simulation. International workshop on defect production, accumulation and materials

performance in irradiation environment, Davos (CH), 2-8 Oct 1996. Unpublished. Abstract available

Singh, B.N., Atomic displacements and defect accumulation during irradiation with energetic particles. In: Kiritani symposium on structural defects in advanced materials. Program and collected abstracts. Kiritani symposium on structural defects in advanced materials, Inuyama, Aichi (JP), 18-20 Dec 1996. (Hiroshima University, Hiroshima, 1996) p. 58

Singh, B.N.; Eldrup, M.; Zinkle, S.J., Damage accumulation in single crystal, polycrystal and cold-worked copper irradiated with fission neutrons at 623 K. In: Program and abstracts for the 18th symposium on effects of radiation on materials. 18. Symposium on effects of radiation on materials, Hyannis, MA (US), 25-27 Jun 1996. (ASTM, Philadelphia, PA, 1996) p. 54

Singh, B.N.; Eldrup, M.; Edwards, D.J.; Toft, P., Effects of bonding and bakeout thermal cycles on pre- and post-irradiation microstructures, physical and mechanical properties of copper alloys. In: Program and abstracts for the 18th symposium on effects of radiation on materials. 18. Symposium on effects of radiation on materials, Hyannis, MA (US), 25-27 Jun 1996. (ASTM, Philadelphia, PA, 1996) p. 59

Singh, B.N.; Garner, F.A.; Edwards, D.J.; Evans, J.H., Influence of nickel and beryllium content on swelling behaviour of copper irradiated with fast neutrons. In: Program and abstracts for the 18th symposium on effects of radiation on materials. 18. Symposium on effects of radiation on materials, Hyannis, MA (US), 25-27 Jun 1996. (ASTM, Philadelphia, PA, 1996) p. 57

Singh, B.N.; Golubov, S.I.; Trinkaus, H.; Serra, A.; Osetsky, Y.N.; Barashev, A.V., Aspects of microstructure evolution under cascade damage conditions. International workshop on defect production, accumulation and materials performance in irradiation environment, Davos (CH), 2-8 Oct 1996. Unpublished. Abstract available

Singh, B.N.; Stubbins, J.F., Fatigue of irradiated copper alloys. In: Program and abstracts for the 18th symposium on effects of radiation on materials. 18. Symposium on effects of radiation on materials, Hyannis, MA (US), 25-27 Jun 1996. (ASTM, Philadelphia, PA, 1996) p. 58

Trinkaus, H.; Singh, B.N.; Formann, A.J.E., Segregation and absorption of cascade induced interstitial loops at dislocations: Effect on initiation of plastic deformation. International workshop on defect production, accumulation and materials performance in irradiation environment, Davos (CH), 2-8 Oct 1996. Unpublished. Abstract available.

Zinkle, S.J.; Fabritsiev, S.A.; Singh, B.N., Radiation hardening in copper alloys. In: Program and abstracts for the 18th symposium on effects of radiation on materials. 18. Symposium on effects of radiation on materials, Hyannis, MA (US), 25-27 Jun 1996. (ASTM, Philadelphia, PA, 1996) p. 53